

Quantum Monte Carlo in the Interaction Representation — Application to a Spin-Peierls Model

A. W. Sandvik

Department of Physics, University of Illinois at Urbana-Champaign, 1110 West Green Street, Urbana, Illinois 61801

R. R. P. Singh

Department of Physics, University of California, Davis, California 95616

D. K. Campbell

Department of Physics, University of Illinois at Urbana-Champaign, 1110 West Green Street, Urbana, Illinois 61801

(June 5, 1997)

I. INTRODUCTION

Over the last two decades, discrete Euclidean path integrals constructed using the so called Trotter decomposition^{1,2} have been widely used as the starting point for quantum Monte Carlo (QMC) simulations of lattice models at finite temperature.^{3–6} In these “worldline” methods,⁶ the discretization $\Delta\tau$ in imaginary time introduces a systematic error in computed quantities, which in principle can be eliminated by carrying out simulations for different discretizations and extrapolating to $\Delta\tau = 0$. The error typically^{2,7} scales as $(\Delta\tau)^2$. However, algorithms can also be constructed which are associated with no inherent systematic errors, thus eliminating the need for multiple simulations and extrapolations. Such a QMC scheme, applicable to the ferromagnetic spin-1/2 Heisenberg model, was first devised by Handscomb as early as in 1961.⁸ This method is based on a series expansion of the density matrix operator $\exp(-\beta\hat{H})$, which in the case of the Heisenberg model can be written in terms of products of permutation operators. Their traces can be evaluated exactly and are positive definite. One can then carry out importance sampling in the space of operator sequences, and obtain results exact to within statistical errors. Handscomb’s method is not directly applicable to other models,⁹ not even for the antiferromagnetic Heisenberg model for which the scheme breaks down due to the non-positive-definiteness of the traces.¹⁰ There was therefore not much follow-up on Handscomb’s pioneering efforts, and there was little progress towards practical QMC algorithms until Suzuki proposed the use of the Trotter formula in this context.² Several methods based on this controlled approximation were subsequently developed.^{5,6,11} Variants of Handscomb’s method were also later developed, for the antiferromagnetic Heisenberg model by Lee *et al.*,¹² and for the XY-model by Chakravarty and Stein,¹³ but this type of simulation scheme was for a long time still perceived as fundamentally limited by its reliance on the special properties of spin-1/2 operators.^{14,15} However, the generalizations of Handscomb’s method developed for $S > 1/2$ spin models by Sandvik and Kurkijärvi,¹⁶ and for 1D Hubbard-type models by Sandvik,¹⁷ have now clearly demonstrated that non-approximate algorithms based on “stochastic series expansion” (SSE) can in principle be constructed for any lattice model. In this scheme, the basic limitation of the earlier formulations of Handscomb’s method is overcome by expanding the traces as diagonal matrix elements in a suitable chosen basis. The importance sampling is then carried out in a space of basis states and operator sequences.^{16,17} In practice, this type of method is of course still limited to models for which a positive definite weight function can be achieved. The cases for which this is possible coincide with those for which the weight is positive definite also in the standard Trotter-based path integral formulations. In fact, despite the different starting points of the two approaches, the SSE configuration space is strongly related to an Euclidean path integral. Many characteristics are therefore shared, including the range of practical applicability, the types of observables accessible for evaluation, and the scaling of the computation time with the system size and the inverse temperature β . The main advantage of SSE is of course the absence of systematic errors. It should be noted that in order to eliminate the Trotter error in worldline calculations, simulations have to be carried out for several sufficiently small discretizations $\Delta\tau$. Since the computation time scales as $1/(\Delta\tau)^3$,¹⁸ the SSE approach can in practice be considerably more efficient than the worldline method in cases where completely unbiased results are needed.

Recently, other approaches to exact QMC algorithms have been proposed. Beard and Wiese succeeded in formulating a worldline algorithm for the spin-1/2 Heisenberg model directly in the $\Delta\tau \rightarrow 0$ limit.¹⁹ Constructed within the framework of a non-Metropolis sampling scheme with global “loop-cluster” updates previously developed by Evertz *et al.*²⁰ (a generalization of the classical cluster spin algorithm²¹), this method also has the added advantage of significantly shorter autocorrelation times. Concurrently, Prokofev, Svistunov and Tupitsyn suggested the use of the standard perturbation expansion as a basis for a QMC path integral.¹⁸ For a finite system at finite temperature the

series converges to an exact result for a finite number of terms. A scheme involving a novel class of local updates was suggested for efficiently sampling the continuous-time paths.

It is clear that the methods by Beard and Wiese¹⁹ and Prokof'ev *et al.*¹⁸ are strongly related to each other, involving the same configuration space of world lines in continuous imaginary time, but differing in the sampling procedures. Continuous-time path integrals also have many properties in common with the SSE sum.^{16,17} Notably, a transition event in imaginary time corresponds directly to the presence of an off-diagonal operator in the SSE operator string. Here we discuss this connection in detail, and introduce a simple modification of the SSE algorithm for simulations in the interaction representation. This formulation can be expected to be more efficient than standard SSE in cases where the diagonal part of the Hamiltonian dominates. In order to explore the properties of the new method, we study the spin-1/2 Heisenberg chain, as well as a spin chain including couplings to dynamic (fully quantum mechanical) phonons. We consider a coupling via a linear modulation of the spin exchange by a local dispersionless oscillator (Einstein phonon). The system undergoes a spin-Peierls (dimerization) transition at zero temperature. A detailed study of the model, and its relevance for understanding the magnetic properties of the recently discovered spin-Peierls compounds GeCuO₃ (Ref. 22) and α' -NaV₂O₅ (Ref. 23), will be presented elsewhere.²⁴ Here we only consider a single set of model parameters, in the general regime expected to be of physical relevance, and illustrate the use of the new method to calculate a variety of physical observables, both at finite temperature and in the limit $T \rightarrow 0$. Based on the results, we conclude that the effects of dynamic phonons cannot be neglected in quantitative descriptions of materials such as those mentioned above.

The outline of the rest of the paper is the following: In Sec. II we review the formalism of the SSE method. The perturbation expansion in the interaction representation and its relation to the SSE series are discussed in Sec. III. In Sec. IV we implement an interaction representation algorithm for the Heisenberg chain, and discuss the performance of the method. In Sec. V we consider the spin-phonon model. Readers interested mainly in the new results for this model are advised to skip directly to the introductory part of Sec. V, and then go directly to the results section V-B. The discussion there does not rely heavily on the previous, more technical parts of the paper. Sec. VI concludes with a summary and outlook for further developments and applications of the new QMC algorithm, in particular to various models including phonons.

II. STOCHASTIC SERIES EXPANSION

Here we review the general formalism of the SSE method, needed as a basis for the discussion in the following sections. More details of the algorithm have been described elsewhere.²⁵ Some recent applications to spin systems and 1D fermion systems are listed in Refs. 26–30.

The starting point for evaluating an operator expectation value at inverse temperature β ,

$$\langle \hat{A} \rangle = \frac{1}{Z} \text{Tr}\{\hat{A} e^{-\beta \hat{H}}\}, \quad Z = \text{Tr}\{e^{-\beta \hat{H}}\}, \quad (1)$$

is to Taylor expand $\exp(-\beta \hat{H})$ and write the traces as sums over diagonal matrix elements in a basis $\{|\alpha\rangle\}$. The partition function is then

$$Z = \sum_{\alpha} \sum_{n=0}^{\infty} \frac{(-\beta)^n}{n!} \langle \alpha | \hat{H}^n | \alpha \rangle. \quad (2)$$

The Hamiltonian is next written as

$$\hat{H} = \sum_{b=1}^M \hat{H}_b, \quad (3)$$

where the operators \hat{H}_b have the “non-branching” property,

$$H_b |\alpha\rangle = h_b(\alpha, \beta) |\beta\rangle, \quad (4)$$

where $|\alpha\rangle$ and $|\beta\rangle$ are both basis states in the chosen representation. Each power \hat{H}^n is now expanded as a sum over all possible products of n of the operators \hat{H}_b . With S_n denoting an index sequence referring to the operators in the product (the operator string),

$$S_n = (b_1, \dots, b_n), \quad b_i \in \{1, \dots, M\}, \quad (5)$$

the partition function becomes

$$Z = \sum_{\alpha} \sum_{n=0}^{\infty} \sum_{S_n} \frac{(-\beta)^n}{n!} \langle \alpha | \prod_{i=1}^n \hat{H}_{b_i} | \alpha \rangle. \quad (6)$$

Eqs. (3) and (4) of course represent a completely general formal device. In practice, one typically chooses the basis so as to make the sum (3) as simple as possible. For example, for the Heisenberg model,

$$\hat{H} = J \sum_{\langle i,j \rangle} \mathbf{S}_i \cdot \mathbf{S}_j, \quad (7)$$

the eigenstates of S_i^z can be chosen; $|\alpha\rangle = |S_1^z, \dots, S_N^z\rangle$. Writing the Hamiltonian as

$$\hat{H} = J \sum_{\langle i,j \rangle} [S_i^z S_j^z + \frac{1}{2}(S_i^+ S_j^- + S_i^- S_j^+)], \quad (8)$$

all the two-spin operators satisfy the requirement (4). For $S = 1/2$, $S_i^+ S_j^- + S_i^- S_j^+$ satisfy (4) and can be considered as a single operator, whereas for $S > 1/2$ the two terms have to be treated as separate operators. For tight-binding fermion or boson models, the real-space occupation number basis is typically chosen. For fermions and hard-core bosons the hopping operator $c_i^+ c_j + c_j^+ c_i$ satisfies (4), whereas for unconstrained bosons the terms again qualify only individually.

For a finite system at finite β , the lengths n of the operator strings contributing significantly to the partition function are restricted to a finite range. In a Monte Carlo simulation of the series expansion, terms (α, S_n) are sampled with a probability proportional to the weight function corresponding to Eq. (6):

$$W(\alpha, S_n) = \frac{(-\beta)^n}{n!} \langle \alpha | \prod_{i=1}^n \hat{H}_{b_i} | \alpha \rangle. \quad (9)$$

Here it will be assumed that $W(\alpha, S_n)$ is positive definite, which of course is not always the case. With a non-positive-definite weight, simulations can in principle still be carried out using $|W|$,⁶ but in practice the statistical fluctuations of calculated expectation values diverge if the positive and negative contributions almost cancel each other, which they do exponentially both with increasing system size and decreasing temperature (the infamous sign problem).^{31,32} As already discussed in the Introduction, this is the most severe limitation of the method — shared also by standard techniques such as the worldline method (in the case of fermions, “determinant methods”¹¹ typically are more effective in dealing with the sign problem³¹). Still, the class of models for which a positive definite W can be achieved is significant enough to motivate the continuing development of more efficient QMC methods for their study.

Proceeding as in the derivation of (6), the numerator in (1) corresponding to a given operator \hat{A} of interest is also expanded. If the expectation value can then be cast into the form

$$\langle \hat{A} \rangle = \frac{\sum_{\alpha} \sum_n \sum_{S_n} A(\alpha, S_n) W(\alpha, S_n)}{\sum_{\alpha} \sum_n \sum_{S_n} W(\alpha, S_n)}, \quad (10)$$

the simulation estimate of $\langle \hat{A} \rangle$ is given by the average of the estimator $A(\alpha, S_n)$ over the sampled configurations:

$$\langle \hat{A} \rangle = \langle A(\alpha, S_n) \rangle. \quad (11)$$

The formally simplest observable within the framework of the SSE method is the internal energy, $E = \langle \hat{H} \rangle$. As in Handscomb’s original formulation, the estimator involves only the power n ;^{8,16}

$$E = -\langle n \rangle / \beta. \quad (12)$$

This, in combination with the expression for the heat capacity,^{8,16}

$$C = \langle n^2 \rangle - \langle n \rangle^2 - \langle n \rangle, \quad (13)$$

shows that the terms contributing significantly are of length $\sim \beta N$ (at low temperatures), where N is the system size. A derivation of (12) will be discussed in the next section.

Already at the level of Eq. (6), the close relationship between SSE and a standard Euclidean path integral is evident. The operator string defines a set of propagated states $|\alpha(p)\rangle$, $p = 0, \dots, n$:

$$|\alpha(p)\rangle \sim \prod_{i=1}^p \hat{H}_{b_i} |\alpha\rangle, \quad |\alpha(0)\rangle = |\alpha\rangle. \quad (14)$$

A nonzero weight (9) implies the periodicity condition $|\alpha(0)\rangle = |\alpha(n)\rangle$. The propagation index p plays a role analogous to imaginary time in a standard path integral. The exact relation to imaginary time can be obtained by deriving an expression for a time-dependent correlation function.¹⁷ Consider two diagonal operators \hat{A}_i and \hat{A}_j . In a given configuration (α, S_n) , their eigenvalues in the states $|\alpha(p)\rangle$ are denoted $a_i[p]$ and $a_j[p]$. One can show that the time-dependent correlation function $C_{ij}(\tau) = \langle \hat{A}_j(\tau) \hat{A}_i(0) \rangle$, where $e^{\tau H} \hat{A}_j e^{-\tau H}$, is given by¹⁷

$$C_{ij}(\tau) = \left\langle \sum_{m=0}^n \binom{n}{m} \frac{\tau^m (\beta - \tau)^{n-m}}{\beta^n} \bar{C}_{ij}(m) \right\rangle. \quad (15)$$

Here $\bar{C}_{ij}(m)$ is a correlator between states separated by m propagations:

$$\bar{C}_{ij}(m) = \frac{1}{n+1} \sum_{p=0}^n a_j[p+m] a_i[p]. \quad (16)$$

The periodicity of the propagated states of course implies that $a_j[p+n] = a_j[p]$. In the equal-time case, only $m = 0$ contributes to (15), and $C_{ij}(0)$ is simply given by $a_i[p] a_j[p]$ averaged over p :

$$C_{ij}(0) = \left\langle \frac{1}{n+1} \sum_{p=0}^n a_j[p] a_i[p] \right\rangle. \quad (17)$$

Eq. (15) shows that an imaginary time separation τ corresponds to a distribution of separations m between propagated states, peaked around $m = n\tau/\beta$. Hence, the propagation index p in the SSE method indeed is closely related to the time in an Euclidean path integral.

As already discussed above, the range of contributing powers n is limited in practice. One can therefore explicitly truncate the series expansion at some maximum power $n = L$, large enough to introduce only an exponentially small, completely negligible error. By inserting $L - n$ unit operators in the operator strings, a configuration space is obtained for which the sequence length formally is *fixed* at L . Defining the unit operator $\hat{H}_0 = I$, the summation over n in (6) is implicitly included in the summation over all sequences S_L , if the range of allowed indices is extended to include also $b_i = 0$. The weight (9) has to be divided by $\binom{L}{n}$, in order to compensate for the number of different ways of inserting the unit operators, resulting in¹⁶

$$W(\alpha, S_L), \frac{(-\beta)^n (L-n)!}{L!} \left\langle \alpha \left| \prod_{i=1}^L \hat{H}_{b_i} \right| \alpha \right\rangle, \quad (18)$$

where n now denotes the number of non-0 indices in S_L . This fixed-length formulation is useful for the construction of an efficient sampling scheme for the sequences. For purposes of measuring operator expectation values, one can still use the expressions discussed above, with the sequences S_n obtained by omitting all the zeros in the generated S_L .

In order to ensure a sufficiently high truncation L , the power n is monitored during the equilibration part of the simulation. If n exceeds some threshold value $L - \Delta_L$, the sequence is augmented with, e.g., $2\Delta_L$ randomly positioned unit operators, corresponding to $L \rightarrow L + 2\Delta_L$. With $\Delta_L \approx L/10$, this procedure typically converges rapidly to a proper L . During a subsequent simulation (of practical duration), n never reaches L . The truncation is therefore no approximation in practice.

The details of the Monte Carlo sampling procedures of course depend on the model under consideration. Here only some general principles will be discussed. The operators \hat{H}_a can be divided into two classes; diagonal and off-diagonal. There are no *a priori* constraints on the number of diagonal operators that can appear in S_L . The probability of a diagonal operator \hat{H}_{dia} at a position p is only determined by the state $|\alpha(p-1)\rangle$ on which it operates. The general strategy for inserting and removing diagonal operators is to attempt substitutions with the unit operator \hat{H}_0 introduced in the fixed-length scheme (note again that \hat{H}_0 is not part of the Hamiltonian):

$$\hat{H}_0 \leftrightarrow \hat{H}_{\text{dia}}. \quad (19)$$

This can be attempted consecutively at all positions in S_L . The weight change needed for calculating the Metropolis or heat-bath acceptance probability involves only the matrix element $\langle \alpha(p-1) | \hat{H}_{\text{dia}} | \alpha(p-1) \rangle$ and the prefactor $(-\beta)^n (L-n)!$, with n changing by ± 1 . With $|\alpha(0)\rangle$ stored initially, the subsequent states can be generated one-by-one as needed during the updating process.

Suitable constants have to be added to the diagonal operators in order to make all the eigenvalues of $-\beta \hat{H}_{\text{dia}}$ positive. According to Eq. (18), the presence or absence of a sign problem then depends only on the off-diagonal operators \hat{H}_{off} . They are associated with various constraints, and cannot be inserted or removed at a single position only. They can always be inserted and removed pairwise. One way to do this is in substitutions with diagonal operators, according to

$$\hat{H}_{\text{dia}}, \hat{H}_{\text{dia}} \leftrightarrow \hat{H}_{\text{off}}, \hat{H}_{\text{off}}^\dagger. \quad (20)$$

In some one-dimensional models, the above types of updates are sufficient for achieving ergodicity. In other cases, more complicated updates are also required (e.g., involving off-diagonal operators forming loops around plaquettes in 2D). The constraints and weight changes associated with local updates involve only operators present in S_L which act on a small number of lattice sites surrounding those directly affected by the update. Typically, this allows for a sampling scheme for which the computation time scales as $N\beta$.¹⁷

III. RELATION TO THE PERTURBATION EXPANSION

In this Section we discuss the general principles of carrying out importance sampling of the standard perturbation expansion in the interaction representation. This starting point for a QMC scheme was recently suggested by Prokof'ev *et al.*¹⁸ We here show that the configuration space of this method is closely related to that of the SSE method. We also derive expressions for several types of observables.

The partition function for a Hamiltonian

$$\hat{H} = \hat{D} + \hat{V}, \quad (21)$$

with a diagonal (unperturbed) part \hat{D} and an off diagonal (perturbing) part \hat{V} is given by the standard time-ordered perturbation expansion in \hat{V} ,

$$Z = \sum_{n=0}^{\infty} (-1)^n \int_0^\beta d\tau_1 \int_0^{\tau_1} d\tau_2 \cdots \int_0^{\tau_{n-1}} d\tau_n \text{Tr} \{ \hat{V}(\tau_1) V(\tau_2) \cdots V(\tau_n) \}, \quad (22)$$

where the time dependence in the interaction representation is $V(\tau) = e^{\tau \hat{D}} V e^{-\tau \hat{D}}$. In the same way as was done in the SSE scheme, \hat{V} can be decomposed into operators that satisfy the requirement (4), now in the basis $\{|\alpha\rangle\}$ where \hat{D} is diagonal:

$$\hat{V} = \sum_{b=1}^{M_V} \hat{H}_b. \quad (23)$$

For a given model, the operators in the above sum are of course a subset of those in the SSE Hamiltonian (3), where we now define the indexing such that all \hat{H}_b with $b > M_V$ are diagonal. An index sequence defining a product of n of the operators \hat{H}_b is defined as before. In order to distinguish the SSE sequence S_n , which contains off diagonal as well as diagonal operators, from the perturbation expansion sequence containing only off-diagonal operators, we denote the latter by T_n :

$$T_n = (b_1, \dots, b_n), \quad b_p \in \{1, \dots, M_V\}. \quad (24)$$

Expanding the trace over diagonal matrix elements gives

$$Z = \sum_{\alpha} \sum_{n=0}^{\infty} \sum_{T_n} \int_0^\beta d\tau_1 \int_0^{\tau_1} d\tau_2 \cdots \int_0^{\tau_{n-1}} d\tau_n W(\alpha, T_n, \{\tau\}), \quad (25)$$

where $\{\tau\}$ is a short-hand for the set of times $\{\tau_1, \dots, \tau_n\}$. The weight is

$$W(\alpha, T_n, \{\tau\}) = (-1)^n \left(e^{-\beta E_0} \prod_{p=1}^n e^{-\tau_p (E_p - E_{p-1})} \right) \left\langle \alpha \left| \prod_{p=1}^n \hat{H}_{b_p} \right| \alpha \right\rangle, \quad (26)$$

where $E_p = \langle \alpha(p) | \hat{D} | \alpha(p) \rangle$.

Now, consider an SSE index sequence $S_n = (b_1, \dots, b_n)$, containing m indices $b_p \leq M_V$, corresponding to m off-diagonal and $n - m$ diagonal operators. Removing all the indices $b_p > M_V$ from S_n results in a valid sequence T_m . We use the notation $[S_n]$ for this “projection” of S_n onto the corresponding T_m ; $[S_n] = T_m$. Since there are no convergence issues for a finite lattice model at finite β , neither for SSE nor for the perturbation expansion, the weights of the two formulations must be related according to

$$\sum_{n=m}^{\infty} \sum_{[S_n]=T_m} W(\alpha, S_n) = \int_0^{\beta} d\tau_1 \int_0^{\tau_1} d\tau_2 \cdots \int_0^{\tau_{m-1}} d\tau_m W(\alpha, T_m, \{\tau\}). \quad (27)$$

Hence, for a given sequence of off-diagonal operators, the time integrals of the perturbation expansion correspond to a summation over all possible augmentations with diagonal operators in the SSE scheme. The equality (27) can be explicitly verified in the extreme case where there are no diagonal operators in \hat{H} , i.e., $\hat{D} = 0$ (for example, the XY-model in the z -component basis). In this case $[S_n] = S_n = T_n$, and the τ -integrals above give $\beta^n/n!$, which is exactly the prefactor of the SSE weight (9).

For a nonzero \hat{D} , the dominant SSE strings contain a finite fraction of diagonal operators, and the integrals in the interaction representation become nontrivial. In constructing a simulation algorithm based on one of these expansions, one hence has to weight the disadvantage of a longer operator string in the SSE scheme against a more complicated weight function in the case of the perturbation expansion. Although the perturbation series integrand is formally simple, it does not appear to be feasible to carry out the time integrals analytically. It is, however, straight-forward to include an importance sampling of the times in the Monte Carlo procedures. It is likely that sampling the perturbation expansion will be more efficient than the SSE algorithm in cases where the diagonal term dominates. The average length of the perturbation expansion is then significantly shorter than the SSE string. Note, however, that the average length of the perturbation expansion has the same scaling $\sim \beta N$ as the SSE string length, as will be discussed further below.

In constructing a function A (the estimator) measuring an operator \hat{A} on the configuration space, symmetries of the space should be taken into account in order to reduce the statistical fluctuations. An evident one is the translational symmetry of periodic (non-random) lattices. Another one is the periodicity in the imaginary time (or SSE propagation) direction, originating from the cyclic property of the trace operation. In the SSE scheme, this is manifested by

$$W(\alpha, S_n) = W(\alpha(p), S_n[p]), \quad p = 0, \dots, n, \quad (28)$$

where $S_n[p]$ is the index sequence obtained by p times cyclically permuting S_n , and $\alpha(p)$ refers to the p times propagated state (14). One can therefore average the measurements over all $p = 0, \dots, n$, an example of which is seen in Eq. (17).

The perturbation expansion involves the imaginary times only in the form of differences. The part of the weight (26) containing the times can be rewritten as

$$e^{-\beta E_0} \prod_{p=1}^n e^{-\tau_p (E_p - E_{p-1})} = \prod_{p=1}^n e^{-E_p \Delta_p}, \quad (29)$$

where $\Delta_p = \tau_p - \tau_{p+1} + \sigma\beta$ is the time difference between the operators at positions $p, p+1$, with $\sigma = 0, 1$ chosen such that $\Delta_p \in [0, \beta]$, and $\tau_n = \tau_0$. Shifting all times by an equal amount δ therefore does not change the weight, provided that the shifted times $\tau_i + \delta$ obey the limits of the time-ordered integration. Hence, $\delta \in [-\tau_n, \beta - \tau_1]$. Cyclically permuting T_n and $\{\tau\}$, and including an appropriate uniform shift δ , is also allowed. We define a permutation of the times with an implicit shift, such that the last time in the permuted sequence is at its lower bound 0. Denoting the p times permuted set $\{\tau(p)\}$, the zero times permuted $\{\tau(0)\}$ hence corresponds to a uniform shift $\delta = -\tau_n$. A permutation with an additional shift is denoted $\{\tau(p) + \delta\}$. Hence we have

$$W(\alpha, T_n, \{\tau\}) = W(\alpha(p), T_n(p), \{\tau(p) + \delta\}), \quad \delta \in [0, \Delta_p]. \quad (30)$$

We now derive expressions for some important types of operator expectation values within the perturbation expansion scheme, and contrast them with those of the SSE formulation.

First, we consider an equal-time correlation function between two diagonal operators,

$$C_{ij} = \langle \hat{A}_j \hat{A}_i \rangle. \quad (31)$$

In the SSE approach, the expansion of $\text{Tr}\{\hat{A}_j \hat{A}_i e^{-\beta \hat{H}}\}$ leads to the same sum as in Eq. (6), with each term multiplied by the eigenvalue $a_i[0]a_j[0] = \langle \alpha | \hat{A}_j \hat{A}_i | \alpha \rangle$. Using the cyclic property (28) then leads to Eq. (17). In the interaction representation, Eq. (30) implies that each cyclic permutation p should be weighted with the time interval Δ_p . Since $\sum_p \Delta_p = \beta$ we get

$$C_{ij} = \frac{1}{\beta} \left\langle \sum_{p=1}^n \Delta_p a_i[p] a_j[p] \right\rangle. \quad (32)$$

This type of expression is, of course, valid for any diagonal operator.

The SSE expression for the static susceptibility,

$$\chi_{ij} = \int_0^\beta d\tau \langle \hat{A}_j(\tau) \hat{A}_i(0) \rangle, \quad (33)$$

can be obtained by integrating the time-dependent expectation value (15) over τ . Alternatively, one can include a source $\sum_j h_j \hat{A}_j$ in the Hamiltonian, and calculate the response function via

$$\chi_{ij} = \left. \frac{\partial \langle \hat{A}_i \rangle}{\partial h_j} \right|_{h_j=0}. \quad (34)$$

The result is^{16,17}

$$\chi_{ij} = \left\langle \frac{\beta}{n(n+1)} \left(\sum_{p=0}^{n-1} a_i[p] \right) \left(\sum_{p=0}^{n-1} a_j[p] \right) + \frac{\beta}{(n+1)^2} \sum_{p=0}^n a_i[p] a_j[p] \right\rangle. \quad (35)$$

In the interaction representation, the derivative (34) applied to $\langle \hat{A}_i \rangle = \sum_p \Delta_p a_i[p] / \beta$ gives

$$\chi_{ij} = \frac{1}{\beta} \left\langle \left(\sum_{p=1}^n \Delta_p a_i[p] \right) \left(\sum_{p=1}^n \Delta_p a_j[p] \right) \right\rangle. \quad (36)$$

Hence, with both methods, there is a simple exact estimator for the static susceptibility. This is important in view of the fact that the discretization can introduce spurious temperature dependences in divergent susceptibilities calculated using standard worldline methods, due to a combination of Trotter errors and numerical integration errors.⁷

A second class of observables easily accessible in SSE as well as real-space path integral formulations is one involving the operators \hat{H}_b present in the Hamiltonian. First, consider a single operator $\langle \hat{H}_b \rangle$. In the SSE formalism, the estimator is

$$\langle \hat{H}_b \rangle = -\langle N(b) \rangle / \beta, \quad (37)$$

where $N(b)$ is the total number of indices $b_i = b$ in the sequence S_n . This formula can easily be derived by noting that the expansion of the numerator $\text{Tr}\{e^{-\beta \hat{H}} \hat{H}_b\}$ leads to a one-to-one correspondence with a subset of the terms in Eq. (6), namely, those for which the last index $b_n = b$. The terms are related by a factor $-n/\beta$, which hence is the contribution to $\langle \hat{H}_b \rangle$ from these partition function configurations. For the terms with $b_n \neq b$ the contribution is zero. Averaging over all cyclic permutations then gives (37). From this result, Eq. (12) for the SSE internal energy estimator follows.

In view of the relation (27) between SSE and the perturbation expansion, we would expect Eq. (37) to be valid also for an off-diagonal operator in the interaction representation scheme. Proceeding as in the SSE derivation, there is again a one-to-one correspondence between the terms of the expansion of $\text{Tr}\{e^{-\beta \hat{H}} \hat{H}_b\}$ and a subset of those in Z . However, the situation is complicated by the fact that, for a given power n , the terms of Z have one more time integration. In order to properly relate the terms to each other, we can formally introduce another integral,

$$\frac{1}{\tau_{n-1}} \int_0^{\tau_{n-1}} d\tau_n = 1, \quad (38)$$

in the expansion of the numerator. Terms of order $n - 1$ are then in a one-to-one correspondence with terms of order n in the partition function (25). The lack of the time-dependent exponential associated with the last operator \hat{H}_b and the factor $1/\tau_{n-1}$ in (38) imply a contribution $-e^{\tau_n(E_n - E_{n-1})}/\tau_{n-1}$, if $b_n = b$. By the cyclic property (30), this can be averaged over the time range Δ_p for each p , giving

$$\langle \hat{H}_b \rangle = -\frac{1}{\beta} \left\langle \sum_{p=1}^n I_b(p) K(p) \right\rangle, \quad (39)$$

where $I_b(p) = 1$ if $b_p = b$ and $I_b(p) = 0$ otherwise. Since $\tau_{p-1} = \tau_p + \Delta_{p-1}$, the contribution if $b_p = b$ is

$$K(p) = \int_0^{\Delta_p} d\tau_p \frac{e^{\tau_p(E_p - E_{p-1})}}{\tau_p + \Delta_{p-1}} = e^{-\Delta_{p-1}(E_p - E_{p-1})} \int_{\Delta_{p-1}}^{\Delta_p + \Delta_{p-1}} dx \frac{e^{x(E_p - E_{p-1})}}{x}. \quad (40)$$

This integral cannot be solved in closed form, except if $E_p - E_{p-1} = 0$. We expect (39) and (37) to be equivalent. Therefore, the average of (40) over all times must give 1. In fact, this is the case already for the average over all $\tau_p \in [\tau_{p+1}, \tau_{p-1}]$, which is equivalent to the average over all Δ_{p-1} in the allowed range $[0, \Delta_{p-1} + \Delta_p]$, with $\Delta_{p-1} + \Delta_p$ kept constant. In doing this averaging, the integral (40) has to be weighted by the relative probability of a given Δ_{p-1} , which according to Eq. (29) is $\sim e^{\Delta_{p-1}(E_p - E_{p-1})}$. The resulting double integral can be solved, with the result

$$K(p) = \frac{\int_0^{\Delta_{p-1} + \Delta_p} dy \int_y^{\Delta_{p-1} + \Delta_p} dx \frac{1}{x} e^{x(E_p - E_{p-1})}}{\int_0^{\Delta_{p-1} + \Delta_p} dx e^{x(E_p - E_{p-1})}} = 1. \quad (41)$$

Thus, we have shown that (39) indeed reduces to the SSE estimator (37). This then also implies that the average length of the perturbation expansion is given by $\langle n \rangle = \beta |\langle \hat{V} \rangle|$, which scales as βN .

In order to derive an expression for an off-diagonal equal-time correlation function of the type

$$F(b_1, b_2) = \langle \hat{H}_{b_1} H_{b_2} \rangle, \quad (42)$$

one can proceed along the same lines as for the single operator considered above. The SSE expression is again formally very simple. Each occurrence in S_n of a pair of indices $b_1 b_2$ gives a constant contribution. Denoting by $N(b_1 b_2)$ the number of such pairs of adjacent operators, the result is¹⁷

$$F(b_1, b_2) = \langle (n - 1) N(b_1 b_2) \rangle / \beta^2. \quad (43)$$

In the interaction representation formalism, the estimator is

$$F(b_1, b_2) = \left\langle \sum_{p=1}^n I_{b_1 b_2}(p - 1, p) K(p - 1, p) \right\rangle, \quad (44)$$

where $I_{b_1 b_2}(p - 1, p) = 1$ if the indices at the adjacent positions $p - 1, p$ are b_1 and b_2 , and zero otherwise. In order to evaluate the contribution $K(n - 1, n)$ from a pair at the last two positions, $n - 1$ and n , we now insert a double integral

$$\frac{2}{(\tau_{n-2})^2} \int_0^{\tau_{n-2}} d\tau_{n-1} \int_0^{\tau_{n-1}} d\tau_n = 1, \quad (45)$$

for a term of power $n - 2$ in the numerator. Performing the appropriate cyclical permutations and time averages analogous to the ones discussed above, the contribution from an arbitrary pair of adjacent operators is

$$K(p - 1, p) = \frac{\int_0^{D_p} dz \int_0^z dy \int_z^{D_p} dx \frac{1}{x^2} e^{x(E_p - E_{p-2})}}{\int_0^{D_p} dy \int_y^{D_p} dx e^{y(E_p - E_{p-1})} e^{x(E_{p-1} - E_{p-2})}}, \quad (46)$$

where

$$D_p = \Delta_{p-2} + \Delta_{p-1} + \Delta_p. \quad (47)$$

Calculating the integrals results in

$$K(p-1, p) = \frac{(E_{p-1} - E_{p-2})/\beta}{1 - \frac{(E_p - E_{p-2})(e^{D_p(E_{p-1} - E_{p-2}) - 1})}{(E_{p-1} - E_{p-2})(e^{D_p(E_p - E_{p-2}) - 1})}}, \quad (48)$$

where special cases such as $E_p - E_{p-2} = 0$ should be treated as limiting values. In order to relate this much more complicated expression to the simple SSE result of a constant contribution $(n-1)/\beta^2$ [Eq. (43)], we note that a typical value of the time interval D_p is $3\beta/n$, and $K(p-1, p) \sim 1/(\beta D_p)$ for D_p small. Hence, a typical value of $K(p-1, p)$ is $\sim n/\beta^2$, i.e. of the same order as the SSE contribution.

The SSE estimator for the static off-diagonal susceptibility,

$$\bar{\chi}_{ij} = \int_0^\beta d\tau \langle \hat{H}_{b_2}(\tau) \hat{H}_{b_1}(0) \rangle, \quad (49)$$

is given by the remarkably simple formula¹⁷

$$\bar{\chi}_{ij} = \langle N(b_1)N(b_2) - \delta_{b_1, b_2} N(b_1) \rangle / \beta. \quad (50)$$

As this expression only involves counting the numbers of indices b_1 and b_2 in the sequence, it must [by the configuration relation, Eq. (27)] be the correct expression in the interaction representation as well [in contrast, the equal-time correlation function discussed above involves pairs of indices, the distributions of which are different in SSE and the interaction representation, due to the diagonal operators present in SSE]. We shall not prove this explicitly here.

The above derivations have clearly shown the close relationships between the SSE configuration space and the continuous time path integral. We note that in cases where the expressions differ, they are generally formally simpler in the SSE case. In this sense, the SSE propagation dimension is a more natural representation of the quantum fluctuations than imaginary time.

At this stage a reader may wonder why the expansion is dominated by such large powers $\langle n \rangle \sim N\beta$, independent of the size of the perturbation, and why is it not dominated by small powers when the perturbation theory converges for an infinite system at $T = 0$. The answer lies in the fact that the stochastic sampling is done for the partition function, for which there is never a convergent expansion as $T \rightarrow 0$ and the size of the system goes to infinity. To clarify the situation, let us assume that the off-diagonal part of the Hamiltonian is multiplied by a perturbation parameter λ . Furthermore, the free energy per unit volume, f , has a convergent expansion

$$f(\lambda) = f_0 + f_1\lambda + O(\lambda^2). \quad (51)$$

Then the series expansion for the partition function for a system of volume N becomes

$$Z = e^{-\beta N f} \propto e^{-\beta N f_1} = \sum_n a_n \lambda^n, \quad (52)$$

with $|a_n| = (\beta N)^n |f_1|^n / (n!)$. It is easy to show that a_n is maximum for $n = \beta N |f_1|$ in agreement with Eq. (37).

An updating scheme for importance sampling of the perturbation series can now be constructed along the lines discussed in the previous section in the context of the SSE method. The differences are only in the weight function, which involves a set of times which also is sampled stochastically. As a pedagogical example, in the following section we develop the details of an algorithm for the simple case of the anisotropic Heisenberg chain. In Sec. V we extend the scheme to include couplings to phonon degrees of freedom (spin-Peierls model).

IV. ALGORITHM FOR THE HEISENBERG CHAIN

Here we describe the details of a perturbation series algorithm developed for the anisotropic $S = 1/2$ Heisenberg chain. We discuss some properties of the method and use exact diagonalization results for small systems as well as known analytical results for the thermodynamic limit to show that very accurate, unbiased results can indeed be produced.

A. Construction of the Algorithm

The model we consider here is defined by the Hamiltonian

$$\hat{H} = J \sum_{i=1}^N [S_i^z S_{i+1}^z + \frac{\Delta}{2} (S_i^+ S_{i+1}^- + S_{i+1}^+ S_i^-)], \quad (J > 0), \quad (53)$$

with periodic boundary conditions. Δ controls the anisotropy, with $\Delta = 1$ corresponding to the isotropic Heisenberg point.

We wish to construct an algorithm in which, as in the SSE scheme, Monte Carlo updates that change the expansion order, n , are accomplished by inserting or removing diagonal operators one at a time, and off-diagonal operators are inserted or removed pairwise in substitutions with diagonal operators. Since there are only off-diagonal operators in the perturbation expansion string, we add constants to the Hamiltonian, and formally consider these as part of the perturbation. For the spin chain at hand we define

$$\hat{H}_{1,b} = -I \quad (54a)$$

$$\hat{H}_{2,b} = S_i^+ S_{i+1}^- + S_{i+1}^+ S_i^-, \quad (54b)$$

and write the perturbation as

$$\hat{V} = \left(\frac{\Delta}{2}\right) \sum_{a=1}^2 \sum_{b=1}^N \hat{H}_{a,b}. \quad (55)$$

For N even, only operator strings with an even number of the off-diagonal operators $\hat{H}_{2,b}$ contribute to the partition function. The weight (26) is hence positive definite. The matrix element of an allowed operator string equals one, and therefore

$$W(\alpha, T_n, \{\tau\}) = (\Delta/2)^n e^{-\beta E_0} \prod_{p=1}^n e^{-\tau_p (E_p - E_{p-1})}. \quad (56)$$

T_n is now for convenience defined as a sequence of index pairs

$$T_n = [a_1, b_1], [a_2, b_2], \dots, [a_n, b_n], \quad (57)$$

with $a_p \in \{1, 2\}$ and $b_p \in \{1, \dots, N\}$ referring to the operator type and lattice bond (nearest-neighbor spin pair), respectively. Using the fixed-length scheme developed for the SSE algorithm, we define $\hat{H}_{0,0} = I$, and insert $L - n$ of these in each string. Taking into account the number of possible insertions then gives

$$W(\alpha, T_L, \{\tau\}) = \frac{(\Delta/2)^n (L - n)! n!}{L!} e^{-\beta E_0} \prod_{p=1}^n e^{-\tau_p (E_p - E_{p-1})}, \quad (58)$$

where n is the number of non-[0, 0] elements in T_L . There are no times associated with the augmentation operators $H_{0,0}$, and the index p in the product therefore refers to the p th non-[0, 0] operator.

The Monte Carlo sampling is based on updates of the types (19) and (20). Using $[a, b]_p$ as an alternative to the notation $[a_p, b_p]$, the update changing the power n by ± 1 is

$$[0, 0]_p \leftrightarrow [1, b]_p, \quad (59)$$

and the simplest update involving off-diagonal operators is

$$[1, b]_{p_1}, [1, b]_{p_2} \leftrightarrow [2, b]_{p_1}, [2, b]_{p_2}. \quad (60)$$

These local updates are sufficient for generating all operator strings for an open chain, or a periodic system in the zero winding number sector. An update changing the winding number will be discussed further below. For a simulation in the canonical ensemble, i.e., with the total magnetization $m = \sum_i S_i^z$ fixed, no further updates of the state $|\alpha\rangle$ are required, since (60) also implies flips of nearest-neighbor spins in the propagated states $|\alpha(p)\rangle$ with $p = p_1, \dots, p_2 - 1$ (here and in the following, the periodicity of the sequence is always implied, so that if $p_1 > p_2$, the affected states are $p_1, \dots, L - 1, 0, \dots, p_2 - 1$). In the grand canonical ensemble, global spin flips changing the magnetization of all the propagated states also have to be carried out.

Fig. 1 shows a graphical representation of a configuration generated for an 8-site isotropic Heisenberg chain. This type of representation emphasizes that in this simulation scheme the ordered sequence of operators is the central

element, and the times formally can be thought of as auxiliary variables associated with the operator positions. In the simulation, only one of the states $|\alpha(p)\rangle$ needs to be stored, since all the other ones are uniquely defined given the operator sequence and can be generated as needed.

First, consider the single-operator update (59). This can be attempted consecutively at all positions $p = 1, \dots, L$ for which $a_p \in \{0, 1\}$. In calculating the Metropolis acceptance probabilities for such updates, the fact that the augmentation operators $\hat{H}_{0,0}$ are not associated with time integrals has to be taken into account. We now define the time difference $\bar{\Delta}_p = \tau(< p) - \tau(\geq p)$, where $\tau(< p)$, and $\tau(\geq p)$ are the times associated with the non- $[0, 0]$ operator closest to p , with position indices $< p$ and $\geq p$, respectively. In a substitution $[0, 0]_p \rightarrow [1, b]_p$, b is chosen at random, and a time τ_p in the range $[\tau(> p), \tau(< p)]$ is generated. In the direction $[1, b]_p \rightarrow [0, 0]_p$, the only action is to replace $[1, b]$ with $[0, 0]$ and discard the time $\tau(p)$. One can easily verify that detailed balance with the distribution (58) is maintained with the following acceptance probabilities (note that the energy difference $E_p - E_{p-1} = 0$ for $[a_p, b_p] = [1, b]$):

$$P([0, 0]_p \rightarrow [1, b]_p) = \min \left[\frac{(\Delta/2)\bar{\Delta}_p N(n+1)}{L-n}, 1 \right] \quad (61a)$$

$$P([1, b]_p \rightarrow [0, 0]_p) = \min \left[\frac{L-n+1}{(\Delta/2)(\bar{\Delta}_p + \bar{\Delta}_{p+1})Nn}, 1 \right]. \quad (61b)$$

The pair substitutions (60) are associated with constraints. In the \rightarrow direction, the first requirement is that $S_b^z[p_1 - 1] = -S_{b+1}^z[p_1 - 1]$. In either direction, an update flips the spins $S_b^z[p]$ and $S_{b+1}^z[p]$ in the states $|\alpha(p)\rangle$ with $p_1 \leq p < p_2$. This implies that there may be no operators $[2, b-1]$ or $[2, b+1]$ present between p_1 and p_2 , and hence that $S_{b+1}^z[p] = -S_{b+1}^z[p]$ for all p in the range affected by the update. The change of the weight (58) in an allowed update at b then depends on the energy differences $E_p - E_{p-1}$ in the local 4-spin substates $|S_{b-1}^z, S_b^z, S_{b+1}^z, S_{b+2}^z\rangle_p$ for $p_1 \leq p \leq p_2$, but only for those p with operators acting on the spins of this substate.

The locality of the constraints and the weight changes allows for a fast updating carried out on *subsequences*.¹⁷ A subsequence b contains all operators $[2, b]$ present in T_L , and those $[1, b]$ operators appearing between antiparallel spins S_b^z and S_{b+1}^z . Information on the constraints imposed by the presence of the nearest-neighbor operators $[2, b-1]$ and $[2, b+1]$ is also part of the subsequence. Operators $[2, b-2]$ and $[2, b+2]$ do not impose constraints, but affect the edge spins of the substates $|S_{b-1}^z, S_b^z, S_{b+1}^z, S_{b+2}^z\rangle$, and therefore also have to be included in the subsequence, so that the acceptance probabilities can be calculated. All the 4-spin substates acted upon by the operators of the subsequences are also stored for this reason. Clearly, subsequences b and b' can be updated independently of each other if $|b' - b| > 2$. Since we normally study chains with N a multiple of 4, we simultaneously construct the subsequences for all bonds separated by 3 other bonds, and update these one by one. Four such partition-updating cycles are then needed for updating all the bonds.

The subsequence information is arranged as follows: The length of subsequence b is denoted L_b , and is the number of operators $[1, b]$, $[2, b]$, $[2, b-2]$, and $[2, b+2]$ present in T_L . These operators are represented by the integers $1-4$, and are stored in lists $A_b(1, \dots, L_b)$. The original positions of these operators in T_L are needed for re-merging the updated subsequences into an updated full sequence, and are stored in lists $P_b(1, \dots, L_b)$. The constraining operators $[2, b \pm 1]$ do not have to be stored. Instead, lists $F_b(1, \dots, n_b)$ are created, such that $F_b(i) = 1$ if there are constraining operators (one or several) in T_L between positions $P_b(i)$ and $P_b(i+1)$, and $F_b(i) = 0$ otherwise. The 4-spin substates are encoded as single integers ($1-16$), and stored in lists $S_b(1, \dots, L_b)$.

For updating the subsequences, we use the scheme introduced in Ref. 17 (other methods are also possible). An attempt to carry out a substitution (60) in a given subsequence b consists of the following steps. A position i_1 such that $F_b(i_1) = 0$ is first chosen at random. One then searches in the forward direction for the first position j for which $A_b(j) = A_b(i_1)$ and $F_b(j) = 1$. This position is the one furthest away from i_1 which can be considered, together with i_1 , in a pair substitution. Note that position $i = 1$ follows $i = L_b$ due to the periodicity, and the search is terminated at $i = i_1 - 1$ if this position is reached (and then $j = i_1 - 1$). During the search, the positions i of all encountered operators $A_b(i) = A_b(i_1)$ are stored. One of these, $i = i_2$, is then selected at random, and the pair $\{A_b(i_1), A_b(i_2)\}$ is replaced by $\{A'_b(i_1), A'_b(i_2)\} = \{2 - A_b(i_1), 2 - A_b(i_2)\}$ with a probability satisfying detailed balance.

The total probability of making a certain pair-substitution is the product of the probability $P_{\text{select}}[A(i_1), A(i_2)]$ of selecting the operators at positions i_1 and i_2 , and the acceptance probability $P_{\text{accept}}[A(i_1)A(i_2) \rightarrow A'(i_1)A'(i_2)]$. One can show that the selection probabilities with the above procedures are the same in both directions,¹⁷ i.e., $P_{\text{select}}[A(i_1), A(i_2)] = P_{\text{select}}[A'(i_1), A'(i_2)]$, if the attempt is *cancelled* with a probability

$$P_{\text{cancel}}[AA \rightarrow A'A'] = 1 - \frac{N(A)}{N(A) + N(A')}, \quad (62)$$

where $N(A)$ and $N(A')$ are the numbers of operators A and A' found between $i = i_1$ and $i = j$ in the search [excluding the first operator $A_b(i_1) = A$]. If the attempt is not cancelled at this stage, a final acceptance probability is calculated on the basis of the weight (58), using the stored substates, and the corresponding states modified due to the replaced operators (obtained by propagating with the updated subsequence segment). The Metropolis acceptance probability is

$$P_{\text{accept}}[AA \rightarrow A'A'] = \min \left[e^{-\beta(E'_0 - E_0)} \prod_{i=p_1}^{p_2} e^{-\tau_{P_b(i)}(E'_i - E'_{i-1} + E_i - E_{i-1})}, 1 \right], \quad (63)$$

where E_i , and E'_i are the eigenvalues of \hat{D} calculated on the substate $|S_{b-1}^z, S_b^z, S_{b+1}^z, S_{b+2}^z\rangle_i$ before and after the operator substitution. Typically, a constraint is encountered already a few steps from the starting position i_1 , and therefore the number of operations required per step is rather small (the cancellation probability (62) is often 0).

For each subsequence, a number of updating attempts proportional to the number of operators in the subsequence is carried out. The average length of the subsequences, and hence the number of operations needed for its updating, is proportional to β at low temperatures. After updating all the subsequences belonging to one out of the four partitions, the updated operators are inserted in the full index sequence, and changes in the local 4-spin substates are copied into the stored full-system state $|\alpha\rangle$. The same procedures are repeated for all four partitions.

In a periodic system, configurations with a non-zero winding number are possible, and cannot be generated by the local updates discussed above. A winding number corresponds to an excess of spin flips in one direction in the course of the propagation with the operator string, i.e., a cyclic permutation of same spins in $|\alpha(L)\rangle$ with respect to those in $|\alpha(0)\rangle$. The winding number can be changed by substituting a “half-ring” of off-diagonal operators by the complementary half-ring according to¹⁶

$$[2, b_1]_{p_1}, [2, b_2]_{p_2}, \dots [2, b_{N/2}]_{p_{N/2}} \leftrightarrow [2, b'_1]_{p_1}, [2, b'_2]_{p_2}, \dots [2, b'_{N/2}]_{p_{N/2}}, \quad (64)$$

where the bonds $b_1, \dots, b_{N/2}, b'_1, \dots, b'_{N/2}$ are a permutation of all the bonds of the periodic lattice. The acceptance rate for this type of update decreases rapidly with increasing system size, due to the increasing number of constraints. In practice, simulations for systems larger than $N \approx 16 - 20$ must be restricted to the sector with zero winding number. The resulting small error is a boundary effect, and vanishes in the thermodynamic limit.³⁸

At high temperatures, simulations can be carried out in the grand canonical ensemble, by including updates of the total magnetization. This is in principle easily achieved by flipping “straight lines” of spins, $S_i^z[0], \dots, S_i^z[L-1]$, which is allowed provided that there are no operators $[2, i-1]$ or $[2, i]$ present in T_L , and the acceptance probability then depends only on the neighbor spins $S_{i-1}^z[0]$ and $S_{i+1}^z[0]$. However, the likelihood of an allowed spin flip decreases rapidly with decreasing temperature, and in practice simulations for $T \lesssim J/10$ have to be carried out in the canonical ensemble.

Finally, we also perform updates of the times $\{\tau\}$ without changes either in the operator string or the states. A single time τ_p can be updated by generating a new time in the allowed range $[\tau_{p+1}, \tau_{p-1}]$ (and $\tau_1 \leq \beta$, $\tau_n \geq 0$), and accepting this with a Metropolis acceptance probability calculated from Eq. (58):

$$P(\tau_p \rightarrow \tau'_p) = \min \left[\exp[(\tau'_p - \tau_p)(E_{p-1} - E_p)], 1 \right]. \quad (65)$$

The typical time separation, and hence the difference $\tau'_p - \tau_p$, scales as $1/N$, and is typically very small. The acceptance rate for these single-time updates is therefore close to 100% in most cases. It is clear that the rate of evolution of $\{\tau\}$ updated this way [in addition to the generation of a random time when inserting an operator in an update (59)], will be very slow for large systems. Therefore, we consider simultaneously updating a whole set of times $\{\tau_{p_1}, \dots, \tau_{p_2}\}$, using the following scheme.

A position p_1 is first chosen at random, and p_2 is chosen as the smaller of $p_1 + n_\tau$ and n , with n_τ a number chosen randomly between 1 and some upper bound m_τ , and m_τ is adjusted so that a reasonable acceptance rate ($\approx 50\%$) is maintained. If the weight would be independent of the times, the distribution of the times would be uniform within the limits of the time ordered integral. If the separation $\tau_{p_2} - \tau_{p_1}$ is not too large, the true distribution will be close to uniform. We therefore attempt to replace the selected set of times by a randomly generated ordered set $\{\tau'_{p_1}, \dots, \tau'_{p_2}\}$, with $\tau'_{p_1} \leq \tau_{p_1-1}$ ($\tau'_{p_1} \leq \beta$ if $p_1 = 1$) and $\tau'_{p_2} \geq \tau_{p_2+1}$ ($\tau'_{p_2} \geq 0$ for $p_2 = n$). The Metropolis acceptance probability for this multi-time update is

$$P(\{\tau_p\} \rightarrow \{\tau'\}) = \min \left[\exp \left(\sum_{p_1}^{p_2} (\tau'_p - \tau_p)(E_{p-1} - E_p) \right), 1 \right]. \quad (66)$$

It is clear that the acceptance rate is essentially determined by the time difference $\tau_{p_2} - \tau_{p_1}$, independently of the system size. In simulations of large systems, the maximum number of simultaneously updated times, $m_\tau + 1$, can

therefore be as high as 10^3 or higher (in many cases, all times can be updated simultaneously). The importance of the multi-time updates will be further discussed below.

We define a Monte Carlo step (MC step) as a sequence of diagonal updates (59) at all positions in T_L , followed by off-diagonal pair updates (60) at all bonds. In a grand canonical simulation, a global flip of each spin is also attempted, and for simulations of small systems with fluctuating winding number “ring updates” (64) are carried out. The number of multi-time updates per MC step is chosen such that, on the average, $\approx 50\%$ of the times are changed. As already noted, an MC step requires of the order of $N\beta$ operations.

B. Performance Tests

We now present some tests of the accuracy of the method. We also briefly address the issues of autocorrelation times, and the equilibration of the simulation. We only consider the spin isotropic Heisenberg case [$\Delta = 1$ in Eq. (53)]. Detailed numerical finite-temperature results for this model have recently been obtained using the SSE method and high-temperature expansions.²⁸

In order to verify that the new QMC algorithm indeed produces results free from detectable systematic errors, we carried out a long simulation of a 12-site system at inverse temperature $\beta = 8$, in the grand canonical ensemble and with fluctuating winding numbers. These results can be directly compared with exact diagonalization data.

A useful internal check of the simulation in the isotropic case is the internal energy calculated in two different ways; from the diagonal nearest-neighbor correlation function as $E_1 = 3\langle S_i^z S_{i+1}^z \rangle$, according to Eq. (17), and from the expectation value of the off-diagonal operators, $E_2 = -(3/2)\langle \hat{H}_{2,i} \rangle$, according to Eq. (37). For the 12-site system at $\beta = 8$, a simulation consisting of 2×10^8 MC steps gave $E_1 = 0.44372(3)$ and $E_2 = -0.44368(2)$, where the numbers within parentheses indicate the statistical errors. The exact result is $E = -0.443697$. Hence, both QMC estimates are accurate to within relative statistical errors of less than 10^{-4} .

We also calculated the static structure factor

$$S(q) = \frac{1}{N} \sum_{j,l} e^{-i(j-l)q} \langle S_j^z S_l^z \rangle, \quad (67)$$

and the corresponding static susceptibility

$$\chi(q) = \frac{1}{N} \sum_{j,l} e^{-i(j-l)q} \int_0^\beta d\tau \langle S_j^z(\tau) S_l^z(0) \rangle. \quad (68)$$

Comparisons with the exact results are presented in Table I. Here the relative accuracy is the highest, $\approx 10^{-4}$, close to $q = \pi/2$. The accuracy is lower close to $q = \pi$, due to the strong antiferromagnetic fluctuations present in the model. At $q = 0$ the accuracy is hampered by the low acceptance rate for the spin flips required in the grand canonical ensemble.

The above results clearly demonstrate that the method in principle is very accurate. We now consider a significantly larger system, and address some practical issues that arise in realistic simulations.

For the Heisenberg chain, a number of exact results are known in the thermodynamic limit. For example, Eggert *et al.* recently calculated the temperature dependence of the uniform magnetic susceptibility $\chi = \chi(q \rightarrow 0)$, using the thermal Bethe Ansatz.³⁹ We here compare their infinite-size result with QMC data for a system with 128 spins. The simulations consisted of $3 - 5 \times 10^7$ MC steps for each temperature. At high temperatures ($T/J \geq 0.1$) the grand canonical ensemble was used, and at lower T the magnetization was kept fixed at $m^z = 0$. In the latter case, we define the uniform susceptibility as $\chi(q_1)$ where q_1 is the smallest non-zero wavenumber; $q_1 = 2\pi/L$. Fig. 2 shows the results. The relative statistical errors are $\approx 10^{-3}$ down to about $T/J = 0.15$, below which the accuracy diminishes due to the low acceptance rate for the grand canonical spin flips. More accurate results could have been obtained by extrapolating to zero wavenumber on the basis of a few points close to $q = 0$, instead of just using $q = 0$. For the grand canonical simulations, the agreement with the exact result is clearly very good, indicating no detectable effects of finite size for $N = 128$ at the temperatures considered. For the canonical ensemble, all results are slightly below than the exact curve, suggesting larger finite-size effects when the magnetization is not allowed to fluctuate (extrapolating to $q = 0$ instead of using q_1 gives a still larger deviation).

In any Monte Carlo simulation, care has to be taken that the equilibrium distribution is reached before measurements are taken. In our algorithm, the cut-off of the perturbation expansion at order L is determined during the equilibration part of the simulation, by monitoring the power n and increasing L whenever n exceeds some threshold fraction of L (typically 90-95%). We have found that an efficient updating of the times $\{\tau\}$ is crucial for achieving a rapid

equilibration. In Fig. 3 we show results for the cut-off versus the simulation time for an $N = 128$ system at $\beta = 8$ for two different ways of updating the times; consecutively updating all the times one-by-one, according to Eq. (65), and collectively updating a whole range of times according to Eq. (66). With single-time updates, the final cut-off $L = 1064$ was reached after approximately 20000 MC steps, whereas the multi-spin updating gave the final L already after 288 steps. In this case, all times were updated simultaneously, with an average acceptance rate of $\approx 70\%$.

Measuring the expectation value of the constant operators $\hat{H}_{1,b}$ also provides for a good check of the equilibration of the sequence length. With $J = 1$, $-2\langle\hat{H}_{1,b}\rangle$ should equal 1, but before equilibrium is reached a calculation using Eq. (37) will deliver a smaller value. In Fig. 3 we also show the evolution of this measurement with MC time, for the two different ways of updating the times. With multi-time updating, the measured values fluctuate around 1 already after 10^3 steps, whereas with single-time updates the result are too low even after 10^5 steps. In both cases, subsequent simulations consisting of 10^7 MC steps gave comparable results for all calculated quantities, with similar statistical errors. Hence, in this case the multi-time update appears to be important for reaching equilibrium, but does not significantly affect the statistics of the simulation otherwise. For larger system the single-time update becomes even less efficient, and it is likely that the multi-time update then will become important also for the statistics of the simulation (i.e., the autocorrelation times of measured quantities).

The efficiency of the updating process in generating independent (uncorrelated) configurations is measured by autocorrelation functions. The optimal frequency for measuring expectation values on the generated configurations is in principle determined by such functions. For a quantity A , the autocorrelation function is defined as

$$\alpha_A(t) = \frac{\langle A(i+t)A(i) \rangle - \langle A(i) \rangle^2}{\langle A(i)^2 \rangle - \langle A(i) \rangle^2}, \quad (69)$$

where $A(i)$ denotes the value of the simulation estimator after i MC steps, and the normalization has been chosen such that $\alpha_A(0) = 1$. For large time separations t , one expects $\alpha_A(t)$ to decay as e^{-t/ξ_A} , where ξ_A is the autocorrelation time. In principle, the long-time dynamics of the simulation is characterized by a single autocorrelation time, i.e., the longest ξ_A . An observable of interest may or may not overlap with the quantity corresponding to this slowest mode. Hence, in practice one will deal with different autocorrelation times for different quantities.

Successive measurements provide independent information only if they are separated by a number of steps sufficiently large for the corresponding autocorrelation function to have decayed substantially. In practise, the decay may be much faster than e^{-t/ξ_A} for short times, and therefore the relevant separation between measurements may be shorter than ξ_A . In general one expects the autocorrelations for observables related to the long-distance properties of the model, such as $S(\pi)$ and $\chi(\pi)$ for the antiferromagnetic Heisenberg chain, to decay slower than those for essentially local quantities such as the energy, or correlation functions away from the wave number of the dominant fluctuations. Fig. 4 shows results for the logarithms of the autocorrelation functions of E , $S(\pi)$, $\chi(\pi)$, and $\chi(0)$ for a 128-site system at $\beta = 8$. For $S(\pi)$ and $\chi(\pi)$, the asymptotic linear decay is the same, as expected, and the autocorrelation time is ≈ 40 MC steps. Note, however, that $\alpha_{S(\pi)}(t)$ decays slightly faster than $\alpha_{\chi(\pi)}(t)$ for short times, which can be understood on account of $S(\pi)$ being an equal time correlation function, whereas $\chi(\pi)$ involves also an integration over imaginary time. This effect becomes even more pronounced at lower temperatures. For $\chi(0)$ the autocorrelation time is considerably longer at this temperature (≈ 80 MC steps), due to the low acceptance rate for the global spin flips. In contrast, at higher temperatures $\chi(0)$ exhibits the shortest autocorrelation time. The autocorrelation function for the energy decays very rapidly, and it is difficult to see a regime with a linear behavior before statistical noise dominates the measurements. One would expect $\alpha_E(t)$ to contain a component of the slowest mode of the simulation, but the overlap may be too small to detect (and hence the effect on the statistics is essentially irrelevant). Clearly, the relevant time scale for measurements of the energy is much shorter than its asymptotic autocorrelation time.

In practice, it is not feasible to measure the autocorrelations in every case. As usual, binning the data, so that a single bin represents a simulation time much longer than the asymptotic autocorrelation time, ensures proper estimates of averages and statistical errors. The only concern then is that the time spent on the measurements should not dominate the simulation. Measuring every 10 – 20 MC steps typically only results in a minor overhead.

V. SPIN-PEIERLS MODEL

The effects of phonons on spin systems in one dimension are of great current interest, in view of the recent discoveries of spin-Peierls transitions in the inorganic compounds GeCuO_3 (Ref. 22) and $\alpha' - \text{NaV}_2\text{O}_5$ (Ref. 23). These materials consist of weakly coupled spin-1/2 chains and dimerize at $T = 14$ K and 36 K, respectively. A variety of experiments have probed their static and dynamic magnetic properties.^{33,34}

To date, most numerical work on spin-Peierls models in 1D has focused on Lanczos exact diagonalization studies of the ground state of dimerized chains, and the finite temperature susceptibility has been calculated using complete

diagonalization of undimerized chains.^{35–37} The QMC approach discussed in this paper should be an excellent tool for detailed non-perturbative studies of spin systems including dynamic, i.e., fully quantum mechanical, phonon degrees of freedom.

Early studies of 1D electronic models including phonons were carried out by Hirsch and Fradkin, using the worldline QMC method with the phonons introduced via their real-space displacement coordinates, in imaginary time discretized with the standard Trotter approximation.⁴¹ We have developed an extension of the Heisenberg algorithm described in the previous Section, with phonons treated in the real-space occupation number basis. We believe that this is a more efficient way to include the phonons, and furthermore the scheme is exact. The same ideas could also easily be implemented within the SSE scheme, but so far we have not done so. The present scheme is likely more efficient than SSE at high temperatures, where the average phonon occupation number is high and dominates the energy. At low temperatures, SSE may in fact be slightly more efficient.

We here restrict ourselves to the perhaps simplest type of spin-phonon coupling, namely, we consider a dispersionless harmonic oscillator with frequency ω_0 at each bond i (Einstein phonons). The exchange interaction between the spins at sites i and $i + 1$ is modulated by the phonon displacement x_i . The Hamiltonian is hence

$$\hat{H} = \sum_{i=1}^N (J + \alpha x_i) \mathbf{S}_i \cdot \mathbf{S}_{i+1} + \omega_0 \sum_{i=1}^N n_i. \quad (70)$$

Here J is the “bare” exchange, α is the spin-phonon coupling, and n_i is the phonon occupation number, given in terms of the phonon creation and destruction operators as $n_i = a_i^\dagger a_i$. We define the phonon displacement operator as

$$x_i = (a_i^\dagger + a_i)/\sqrt{2}, \quad (71)$$

and hence absorb in the coupling α the mass and spring constant of the oscillator. The oscillator potential corresponding to the definition (71) is $V(x) = \omega_0 x^2/2$.

We remark that the linear coupling is not completely realistic, since it can lead to negative (ferromagnetic) spin-spin couplings if the fluctuations are large. In the low temperature regime this does not occur, and the model should then be a good starting point for understanding the effects of phonons in real quasi-1D spin systems.

Augier and Poilblanc⁴⁰ have recently studied a model related to the Hamiltonian (70). They included only the phonons with momentum $q = \pi$, which are the ones forming a condensate in the dimerized state, and carried out $T = 0$ Lanczos exact diagonalization in a space with a restricted number of these phonons. They found quantitative changes in the behavior from that of a statically dimerized system. Here we will show that the $q \neq \pi$ phonons are also important at finite temperature, in particular the $q = 0$ ones which lead to a temperature dependent effective spin-spin coupling.

A. Algorithm

In a simple modification of the Heisenberg algorithm described in the previous Section, we now have additional phonon occupation number operators in the unperturbed Hamiltonian;

$$\hat{D} = J_0 \sum_{b=1}^N S_b^z S_{b+1}^z + \omega_0 \sum_{b=1}^N n_b. \quad (72)$$

We write the perturbation $\hat{V} = \sum_{a,b} \hat{H}_{a,b}$ in terms of the following operators:

$$\hat{H}_{1,b} = -J_0/2 \quad (73a)$$

$$\hat{H}_{2,b} = (J_0/2)(S_b^+ S_{b+1}^- + S_{b+1}^+ S_b^-) \quad (73b)$$

$$\hat{H}_{3,b} = (\alpha/2\sqrt{2})(S_b^+ S_{b+1}^- + S_{b+1}^+ S_b^-) a_b^\dagger \quad (73c)$$

$$\hat{H}_{4,b} = (\alpha/2\sqrt{2})(S_b^+ S_{b+1}^- + S_{b+1}^+ S_b^-) a_b \quad (73d)$$

$$\hat{H}_{5,b} = (\alpha/\sqrt{2})(S_b^z S_{b+1}^z - \frac{1}{4}) a_b^\dagger \quad (73e)$$

$$\hat{H}_{6,b} = (\alpha/\sqrt{2})(S_b^z S_{b+1}^z - \frac{1}{4}) a_b \quad (73f)$$

$$\hat{H}_{7,b} = (\alpha/2\sqrt{2}) a_b^\dagger \quad (73g)$$

$$\hat{H}_{8,b} = (\alpha/2\sqrt{2}) a_b. \quad (73h)$$

The definitions of $\hat{H}_{5,b}$ and $\hat{H}_{6,b}$ contain off-diagonal operators $\sim a_b^\dagger$ and $\sim a_b$, which are not present in the original Hamiltonian. They have been included in order to make the weight function positive definite. They also induce a constant shift in the oscillators, which has no effect other than shifting the value of J by an amount proportional to α^2 . The operators $\hat{H}_{7,b}$ and $\hat{H}_{8,b}$ have been included in the Hamiltonian in order to enable straight-forward measurements of correlation functions of the displacement operators x_b , which are off-diagonal in the chosen representation and hence must be measured using expressions such as Eqs. (44) and (50) [the prefactor in (73g) and (73h) is chosen for convenience, but is in principle arbitrary]. Again, these operators just shift the effective value J and therefore do not affect the physics of the model.

In order to compensate for the shift induced by the added operators, we define the spin-spin coupling in Eqs. (73b) and (72) with a constant $J_0 \neq J$, determined such that the new bare coupling $J = 1$ (i.e., its value in the absence of the spin-phonon coupling $\alpha \sum_i x_i \mathbf{S}_i \cdot \mathbf{S}_{i+1}$, which in turn induces an additional shift which is part of the physics of the model). For each bond, the added operators equal $(3\alpha/4)x_b$. Thus the shifted oscillator potential is $V'(x) = \omega_0(x - 3\alpha/4\omega_0)^2/2$. The actual bare value of J is then

$$J = J_0 + \frac{3\alpha^2}{4\omega_0}, \quad (74)$$

and we therefore choose $J_0 = 1 - \frac{3}{4}(\alpha/J)(\alpha/\omega_0)$ and $J = 1$. If we do not want to deal with negative values of J_0 , this implies that the maximum coupling constant we can study, for a given ω_0 , is $\alpha_{\max} = 2(J\omega_0/3)^{1/2}$, which is probably not a serious restriction for realistic situations. We can relax the restriction by choosing a smaller prefactor in the definition of $\hat{H}_{7,b}$ and $\hat{H}_{8,b}$, or leaving out these operators altogether (which can be done if no phonon correlation functions need to be measured in the simulation). We note that in principle one can use $J_0 < 0$ and avoid the coupling constant restriction. However, this causes a sign problem due to frustration. The standard way of treating the phonons, in the representation where the displacements x_i are diagonal,⁴¹ avoids this by enforcing a positive coupling. This corresponds to including non-linear terms in the oscillator potential and/or the coupling, and hence modifies the model itself. This clearly makes sense from the point of view of modeling real materials. Including nonlinear terms that strictly enforce a positive sign appears to be complicated with our simulation scheme, and therefore the standard method is likely preferable in cases where this would be necessary. Note, however, that including “simple” nonlinear terms in the oscillator potential should be possible, as long as they do not cause a sign problem.

It is now a simple matter to include Monte Carlo updates involving the operators $\hat{H}_{a,b}$ with $a = 3, \dots, 8$ in the Heisenberg simulation scheme developed in the previous Section. As before, we denote by $\hat{H}_{0,0}$ a unit operator, not part of the Hamiltonian, introduced in order to fix the length of the index sequence to L . The operator string matrix element in the weight function, Eq. (26), is more complicated than before, since the matrix elements of the phonon operators depend on the occupation numbers n_b ;

$$\begin{aligned} a_b |n_b\rangle &= \sqrt{n_b} |n_b - 1\rangle, \\ a_b^\dagger |n_b\rangle &= \sqrt{n_b + 1} |n_b + 1\rangle. \end{aligned} \quad (75)$$

Hence, changes in the matrix element of T_L have to be evaluated in pair substitutions involving phonon operators. Apart from this, the methods we use for updating the configurations are very similar to the Heisenberg case, and we shall therefore merely list the types of substitutions carried out and only very briefly comment on their implementation.

As before, the update changing the expansion power n is $[0, 0] \leftrightarrow [1, b]$, with acceptance probabilities given by Eq. (61) [with J_0 in place of Δ]. The pair substitutions can be divided into two classes. A substitution of the first type is only accompanied by changes in the spin states. We use the following ones:

$$[1, b], [1, b] \leftrightarrow [2, b], [2, b] \quad (76a)$$

$$[3, b], [4, b] \leftrightarrow [5, b], [6, b] \quad (76b)$$

$$[4, b], [3, b] \leftrightarrow [6, b], [5, b]. \quad (76c)$$

These updates are again carried out with T_L partitioned into one out of four sets of subsequences. The other updates cause changes only in the phonon states. These are

$$[2, b], [2, b] \leftrightarrow [3, b], [4, b] \quad (77a)$$

$$[3, b], [4, b] \leftrightarrow [4, b], [3, b] \quad (77b)$$

$$[1, b], [3, b] \leftrightarrow [5, b], [2, b] \quad (77c)$$

$$[1, b], [4, b] \leftrightarrow [6, b], [2, b] \quad (77d)$$

$$[2, b], [5, b] \leftrightarrow [3, b], [1, b] \quad (77e)$$

$$[2, b], [6, b] \leftrightarrow [4, b], [1, b] \quad (77f)$$

$$[5, b], [6, b] \leftrightarrow [7, b], [8, b] \quad (77g)$$

as well as the ones obtained from these by permuting operators both on the left and the right. Since the oscillators are independent (i.e., we have not included phonon-phonon couplings), these updates can be carried out independently for all bonds, with T_L partitioned into N subsequences.

For small systems, we also carry out “ring” updates changing the winding number according to Eq. (64). Global flips of single spins can again be carried out only at relatively high temperatures, thus necessitating the use of a canonical ensemble for the spin sector at lower temperatures. For the phonons, the algorithm is automatically grand canonical at any temperature, since the phonon number is not conserved. We do, however, also include global fluctuations of the number of phonons at each bond. For this purpose, we monitor (during equilibration) the average number of phonons per oscillator, $\langle n_b \rangle$, and attempt adding or subtracting between 1 and $\sqrt{\langle n_b \rangle}$ phonons at a time.

Since the number of phonons is unbounded (in practice the largest number sampled is limited, but can be very large at high temperatures), we cannot test the QMC program against exact diagonalization results with the full phonon space included. However, we have compared results with exact diagonalizations for a 4-site chain with the number of phonons per oscillator restricted to less than or equal to two. This restricted case already encompasses all the elements of the simulation algorithm, and hence we can conclude that our program generates results exact within statistical errors.

B. Results

We shall here only present some selected illustrative results for the spin-Peierls model, deferring to a separate publication a detailed discussion of the physics of the model, and its relevance in interpreting various experimental results for quasi-1D spin systems.²⁴ The main purpose here is to give an impression about the kind of detailed information that can be extracted using the new QMC algorithm. We do, however, also point out some important model features of experimental relevance that can be inferred already from the results obtained here.

We note that in the adiabatic limit $\omega_0 \rightarrow 0$, the model should dimerize for any α .⁴² The situation for finite frequency is still not completely settled. For the case of noninteracting spinless fermions, which is equivalent to the XY spin chain, Hirsch and Fradkin found numerical evidence that a critical phonon coupling is required for a dimerization to occur. We here consider a phonon frequency $\omega_0 = J/10$, and a coupling $\alpha = J/4$. Our low-temperature results show that the system is dimerized at $T = 0$ for these parameters. Based on their exact diagonalization study including the $q = \pi$ phonons only, Augier and Poilblanc⁴⁰ suggested a coupling $\alpha/J \approx 0.38$ (after adjusting for a difference $\sqrt{2}$ in definitions) and a bare frequency $\omega_0/J = 0.3$ for describing α' -NaV₂O₅. Hence, the case considered here is closer to the adiabatic limit, and the spin-phonon coupling is slightly weaker. This is still a regime that can be expected to be of relevance for real materials. As we will see, our bare coupling J is in fact renormalized to a slightly higher value due to $q = 0$ phonons, so that our effective phonon frequency and coupling are somewhat lower in units of the effective spin-spin coupling.

We present simulation results for a wide range of finite temperatures, including low enough T to give the ground state for all practical purposes. Systems with up to 128 sites are considered, and a simulation typically consisted of $1 - 2 \times 10^7$ MC steps. At high temperatures ($T/J \geq 0.125$), we used the grand canonical ensemble for the spins, and at lower T we had to restrict ourselves to the canonical ensemble with $m^z = 0$, due to the low acceptance rate for global spin flips. For the relatively large lattices considered, the effects of this restriction are minor. As already noted, the simulation algorithm is automatically grand canonical for the phonons, and we have found no practical problems with the ability of the phonon numbers to fluctuate effectively.

The spin-phonon coupling causes an average uniform displacement $\langle x_i \rangle > 0$ of the oscillators, due to the energy lowering realized by increasing the average coupling, $J \rightarrow J + \alpha \langle x_i \rangle = J_{\text{eff}}$, balanced by the increased potential energy of the oscillator. Hence, the spin-Peierls system is characterized by a temperature dependent effective spin-spin coupling $J_{\text{eff}}(T)$. Fig. 5 shows our QMC results for the effective coupling, along with its RMS fluctuation, defined as

$$\sigma(J_{\text{eff}}) = \alpha \sqrt{\langle x_i^2 \rangle - \langle x_i \rangle^2}. \quad (78)$$

As already noted, the relevance of the model to real materials is likely limited to the regime where J_{eff} rarely fluctuates to negative values. The results of Fig. 5 indicate that, for the model parameter considered here, this is the case for $T/J \lesssim 1$, where $J_{\text{eff}} > \sigma(J_{\text{eff}})$.

At low temperatures, the long-wavelength spin susceptibility shows the behavior expected for a dimerized spin chain. Fig. 6 shows results for $\chi(q)$ for $q < \pi/2$. The behavior changes rapidly between inverse temperatures $\beta = 16$

and 64, from having only a very weak q -dependence in the $q \rightarrow 0$ regime in the former case, to a rapid suppression in the latter case. This clearly shows the presence of a spin gap. There is only a minor change going to $\beta = 128$, indicating that the system is essentially in its ground state at this inverse temperature. In order to accurately extract the uniform susceptibility $\chi(q \rightarrow 0)$, it is necessary to extrapolate to $q = 0$ using 2–4 low- q points. This procedure is of sufficient accuracy in the interesting intermediate temperature regime where the susceptibility drops rapidly.

The uniform susceptibility is one of the most important experimentally measurable quantities. It is often used to estimate the Heisenberg spin-spin coupling. In comparing results for the spin-Peierls model with the Heisenberg chain, it is natural to measure the temperature in units of the effective coupling at $T = 0$, which we denote $J_{\text{eff}}(0)$. We here have $J_{\text{eff}}(0) \approx 1.273$ [see Fig. 5]. Susceptibilities calculated in the simulation, where the bare exchange $J = 1$ is used to set the temperature scale, then also have to be adjusted by this factor since the definition (68) contains the inverse temperature. Hence, unless stated otherwise, we now define $\beta = J_{\text{eff}}(0)/T$, and give the susceptibility in units of $1/J_{\text{eff}}(0)$.

In Fig. 7 we compare the uniform susceptibility of the spin-Peierls model with the exact Heisenberg result.³⁹ There is a significant shift in both the peak position and the amplitude. Both can be understood on the basis of the reduced antiferromagnetism due to the fluctuations induced by the phonons. There are no signs of a suppression of the susceptibility for $T/J_{\text{eff}}(0) \gtrsim 0.1$, below which there is a sudden, very rapid drop. Above this drop, we find that the shape of the temperature dependence of χ can be quite well fit to the result for the Heisenberg chain without phonons, but with an exchange $J_{\text{fit}} < J_{\text{eff}}(0)$, as also indicated in the figure. The over-all magnitude of the susceptibility is then found to be lower than for a Heisenberg chain with this exchange $J = J_{\text{fit}}$. In terms of an effective Landee g -factor (i.e., the value of the g -factor one would deduce under the incorrect assumption that the system is described by a Heisenberg chain), which is 2 for an ideal $S = 1/2$ Heisenberg chain, this implies $g_{\text{fit}} < 2$. For the parameters used here, we find $J_{\text{fit}} \approx 0.82J$ and $g_{\text{fit}} \approx 1.86$. This is interesting, since experimentally it is sometimes found that the g -factor extracted from the susceptibility fit is less than 2, whereas one would in fact expect⁴³ a g -factor slightly larger than 2. For example, Eggert was able to fit well experimental susceptibility data for Sr_2CuO_3 with the Heisenberg $\chi(T)$,⁴⁴ but the g -factor corresponding to the fit is as low as 1.6, and this seeming discrepancy has not been explained. Based on our results presented here, we propose that the apparent g -factor reduction may be at least partially due to phonons. Additional calculations for various phonon frequencies and couplings are underway to further investigate this possibility. Note that the susceptibility of the spin-Peierls model deviates significantly from the Heisenberg $\chi(T)$ also if one considers a temperature-dependent energy scale $J_{\text{eff}}(T)$ instead of the fixed scale $J_{\text{eff}}(0)$ used above, as shown in the inset of Fig. 7. The shift in the peak position remains, and there is a regime where the phonons cause a significant susceptibility enhancement. This shows that the effects of the phonons cannot be simply captured by a mapping to a Heisenberg chain with a temperature-dependent exchange equal to the average coupling $J_{\text{eff}}(T)$ of the model, i.e., the fluctuations in $J_{\text{eff}}(T)$ must be taken into account. These issues will be discussed in more detail elsewhere.²⁴

The effects of the phonons on the antiferromagnetism can be seen directly in the staggered susceptibility, graphed in Fig. 8. For the Heisenberg chain $\chi(\pi) = D \ln^{1/2}(\Lambda/T)/T$ at low temperatures, where the constants have been estimated as $D \approx 0.32$ and $\Lambda \approx 6$.²⁸ For the gapped spin-Peierls model we should have $\chi(\pi) \rightarrow \text{constant}$. We find here that there is a maximum in $\chi(\pi)$ approximately at the same temperature at which the rapid drop in the uniform susceptibility is seen [the staggered structure factor $S(\pi)$ exhibits a similar maximum]. This behavior is distinctively different from that of a gapped system with fixed values of the exchange couplings, such as a statically dimerized chain, for which $\chi(\pi)$ simply saturates at a value set by the gap. In the presence of dynamic phonons the staggered correlations among the instantaneous spin-spin couplings only build up gradually as T is lowered, and therefore the antiferromagnetic spin correlations can initially grow stronger than what they will eventually be in the statically dimerized $T = 0$ state. Experimentally, this may have implications for NMR experiments, which probe the low-frequency dynamic spin-spin correlations. The NMR rates for models including phonons should be accessible using the same numerical techniques (QMC and maximum-entropy analytic continuation) that have recently been used for the standard Heisenberg chain.^{27,28}

The phonon correlations are also interesting, and can give some indirect information on the dynamics as well. We define the static phonon structure factor and susceptibility according to

$$S_x(q) = \frac{\alpha^2}{N} \sum_{j,l} e^{-i(j-l)q} \langle (x_j - \langle x \rangle)(x_l - \langle x \rangle) \rangle, \quad (79a)$$

$$\chi_x(q) = \frac{\alpha^2}{N} \sum_{j,l} e^{-i(j-l)q} \int_0^\beta d\tau \langle (x_j(\tau) - \langle x \rangle)(x_l(0) - \langle x \rangle) \rangle. \quad (79b)$$

We expect both to develop peaks at $q = \pi$ at low temperatures, signaling the dimerization instability. Fig. 9 shows results at several temperatures. At high temperatures, both $S_x(q)$ and $\chi_x(q)$ are almost independent of q and increase

with increasing temperature. This reflects the behavior of (almost) independent harmonic oscillators. At lower temperatures, the expected peaks at $q = \pi$ develop. In the high and intermediate temperature regime ($T \gtrsim \omega_0$) graphed in Fig. 9, $T\chi_x(q) = S_x(q)$ within statistical errors. Hence, at these temperatures the phonon dynamics is for all wavelengths dominated by the first Matsubara frequency and is thus essentially classical. Note that the phonon susceptibilities have considerably smaller statistical errors than the structure factors. This is contrary to the situation for the spin structure factor and susceptibility, which are calculated using the diagonal S_i^z operators. This counterintuitive feature of the QMC method can be traced to the simple form of the off-diagonal susceptibility estimator, Eq. (50).

The static phonon structure factor and susceptibility can be related to the dynamic real-frequency phonon correlation function (or spectral function) $A(q, \omega)$ through sum rules. We define the spectral function as

$$A(q, \omega) = \alpha^2 \sum_{j,l} e^{iq(j-l)} \int_{-\infty}^{\infty} dt e^{-i\omega t} \langle x_l(t) x_j(0) \rangle. \quad (80)$$

From the Lehmann representation one can derive the following sum rules in the standard way:⁴⁵

$$S_x(q) = \frac{1}{\pi} \int_0^{\infty} (1 + e^{-\beta\omega}) A(q, \omega) \quad (81a)$$

$$\chi_x(q) = \frac{2}{\pi} \int_0^{\infty} (1 - e^{-\beta\omega}) \frac{1}{\omega} A(q, \omega). \quad (81b)$$

At $T = 0$, these sum rules can be used to obtain an *upper bound for the lowest phonon excitation of momentum q* , according to

$$w_{\min}(q) \leq 2S_x(q)/\chi_x(q). \quad (82)$$

In the case of a single sharp phonon mode, $2S_x(q)/\chi_x(q)$ is the exact excitation energy. This bound has recently been used to extract spin and charge velocities of 1D electronic models from QMC data.³⁰ Here we demonstrate its use for the phonon spectrum. Fig. 10 shows results for a 128-site system at a low temperature, $T = J/128$. For long wavelengths, the calculated bound is at the bare phonon frequency $\omega_0/J = 0.1$ within statistical errors, indicating a very weak effective coupling of these phonons to the spin system. For $q \rightarrow \pi$, there is a clear reduction, as expected due to the softening of the $q = \pi$ mode in a system that spontaneously dimerizes. In an infinite system, the $T \rightarrow 0$ bound $2S_x(\pi)/\chi_x(\pi) \rightarrow 0$ since a static dimerization implies the classical relation $\chi_x(\pi) = \beta S_x(\pi)$. For a finite system, there is always a gap (decreasing with increasing size) to the lowest phonon excitation and both $S_x(q)$ and $\chi_x(q)$ therefore saturate at finite values for all q . For $q \neq \pi$, the results shown in Fig. 10 are saturated, but $\chi(\pi)$ (but not $S_x(\pi)$) still grows with decreasing T and the actual $T = 0$ bound is therefore considerably lower than that in the figure.

We now calculate the size of the Peierls distortion. In the dimerized state the average displacement alternates between even and odd sites; $\langle x_i \rangle = \langle x \rangle \pm \delta$. Hence, the $T = 0$ staggered phonon structure factor is, for large system sizes N , given by

$$S_x(\pi) = \alpha^2 \delta^2 N. \quad (83)$$

Fig. 11 shows $S_x(\pi)$ versus the inverse temperature J/T for several system sizes. As expected, the saturation takes place at a temperature which decreases with increasing system size. The results for $N = 32$ and $N = 128$ obey Eq. (83) quite accurately, the ratio of the saturated values being ≈ 4 . For $N = 8$ the value is considerably lower, indicating much larger fluctuations in this small system. Using the $N = 128$ result with Eq. (83) gives a dimerization $\alpha\delta \approx 0.13$, i.e., the effective alternating average exchange is $J_i = J_{\text{eff}}(0)[1 \pm \Delta_J]$, with $\Delta_J \approx 0.10$.

The main purpose here has been to illustrate how various physical quantities are accessible with the new QMC algorithm. We have therefore not discussed how our results compare to, e.g., mean-field theory and previous numerical calculations including only the $q = \pi$ phonon mode.⁴⁰ These important issues will be addressed in a future publication.

VI. SUMMARY AND DISCUSSION

In this paper we have introduced a new quantum Monte Carlo algorithm based on the standard perturbation expansion in the interaction representation. This starting point was first suggested by Prokofev *et al.*¹⁸ Our implementation of the sampling of the series is different and is essentially an adaptation of procedures previously developed for the Stochastic Series Expansion algorithm.¹⁷ We have shown that the SSE sum and the continuous imaginary time path integral are in fact very strongly related to each other.

As in the SSE scheme, the central element of the new method is the ordered sequence of operators. In the interaction representation formulation developed here, time enters in the form of auxiliary variables associated with the sequence positions. The operator updates leading to changes in the particle propagation paths (kink-antikink creation and annihilation, in the language of Prokofev *et al.*¹⁸) are carried out via substitutions of pairs of off-diagonal and constant operators, with the time field held fixed. An efficient procedure for collective updating of whole segments of the time field was introduced. We also derived expressions for several types of important operator expectation values, and compared these with the corresponding expressions previously obtained within the SSE scheme.

Not having carried out comparisons with the procedures suggested by Prokofev *et al.*, we do not know which of the two sampling schemes is more efficient — most likely this is model dependent. We believe that the method discussed here is more efficient than the SSE approach in cases where the diagonal part of the Hamiltonian dominates the internal energy. However, the weight function is simpler in the SSE case, and again it is not easy to make a general statement of exactly when the advantages of new method become significant.

We note that the loop-cluster algorithm, invented by Evertz *et al.*,²⁰ has recently been used with considerable success in studies of various spin-1/2 Heisenberg systems,⁴⁶ in particular in the exact formulation developed by Beard and Wiese.¹⁹ Variants of the loop algorithm have also been suggested for the 1D Hubbard model,⁴⁷ and for $S > 1/2$ spin chains.⁴⁸ However, physics results for these cases have not yet been presented. Although its performance for the Heisenberg model can be considered spectacular (however, for some quantities more accurate results have actually been obtained with the SSE method⁴⁹), it is not clear how the loop algorithm will fare with more complicated models, such as spin-phonon models. It is known to break down completely in some cases.²⁰ In contrast, the stochastic series expansion algorithm and the perturbation series schemes are in principle completely general and are practically useful for a wide range of models for which the sign problem can be avoided.

As a demonstration of the power of the new method, we have implemented it for studies of a spin-Peierls model. We considered oscillators associated with the bonds, coupled to the spins via a linear modulation of the exchange. Unlike earlier studies of 1D electronic models coupled to phonons,⁴¹ we used the occupation number basis also for the phonons. The new QMC algorithm is ideally suited for this type of models, since the bare phonon part of the Hamiltonian is diagonal. The initial results presented here for the spin-Peierls chain indicate that reliable results can be obtained with modest computer resources (the simulations were run on mid-range workstations). The method should be very useful for resolving issues related to the effects of dynamic phonons on the physics of the recently discovered inorganic spin-Peierls compounds, as well as other quantum spin systems. Work along these lines is in progress.²⁴ 1D itinerant electronic models of the Hubbard and t - J types including phonons can also be studied using the procedures developed here. We also believe that studies of spin-phonon models in higher dimensions are feasible with our new method.

The results presented here for the spin-Peierls model already indicate some important consequences of dynamic phonons at finite temperature. The type of phonons considered here naturally lead to a temperature dependent effective spin-spin coupling. We found that the uniform magnetic susceptibility still has a shape rather similar to that of the Heisenberg chain in a sizable regime close to the susceptibility maximum often used to extract the size of the exchange coupling from experimental data. However, both the value of J and the g -factor extracted from a fit are reduced relative to a Heisenberg chain with a coupling equal to the average coupling of the spin-phonon model. We propose that this dynamic effect may at least partially be the reason for the reduced g -factor found in some quasi-1D systems.⁴⁴ Furthermore, these results cast some doubts on the validity of detailed extractions^{35,37} of the nearest-neighbor and next-nearest-neighbor couplings in GeCuO_3 from fits of exact diagonalization data of frustrated Heisenberg chains to susceptibility measurements. It is likely that the couplings extracted from such fits do not directly correspond to the true spin-spin couplings of the system, but are influenced by the temperature dependence of the couplings as well as their fluctuations, as discussed above. Interchain couplings likely also have some non-negligible effects on the susceptibility. Unfortunately, the QMC approach introduced here does not allow for studies of frustrated systems (at least not at very low temperatures), due to sign problems. Since α' - NaV_2O_5 is not expected to be frustrated,^{23,34} we believe that detailed experimental studies of this material in combination with finite- T QMC studies will be of key importance in clarifying the microscopic physics of the spin-Peierls materials.

VII. ACKNOWLEDGMENTS

This work is supported by the National Science Foundation under Grants DMR-89-20538 (AWS and DKC) and DMR-96-16574 (RRPS).

- ¹ H. F. Trotter, Proc. Am. Math. Soc. **10**, 545 (1959).
- ² M. Suzuki, Prog. Theor. Phys. **56**, 1454 (1976).
- ³ For reviews of QMC methods, see, e.g. D. Scalapino, in Proceedings of International School of Physics “Enrico Fermi”, 1987, ed. by R. A. Broglia and J. R. Schrieffer (Elsevier Science Pub., 1988); W. Von Der Linden, Phys. Rep. **220**, 53 (1992); A. W. Sandvik, in *Strongly Correlated magnetic and Superconducting Systems*, Proceedings of the 1996 El Escorial Summer School, ed. by G. Sierra and M. A. Martin Delgado (Springer-Verlag, to be published 1997).
- ⁴ M. Suzuki (ed.), *Quantum Monte Carlo methods in Equilibrium and Nonequilibrium Systems*, (Springer-Verlag Berlin, 1987).
- ⁵ M. Suzuki, S. Miyashita, and A. Kuroda, Prog. Theor. Phys. **58**, 1377 (1977); M. Barma and B. S. Shastry, Phys. Rev. B **18**, 3351 (1977); J. J. Cullen and D. P. Landau, Phys. Rev. B **27**, 297 (1983).
- ⁶ J. E. Hirsch, R. L. Sugar, D. J. Scalapino and R. Blankenbecler, Phys. Rev. B **26**, 5033 (1982).
- ⁷ R. M. Fye, Phys. Rev. B **33**, 6271 (1986).
- ⁸ D. C. Handscomb, Proc. Cambridge Philos. Soc. **58**, 594 (1962); **60**, 115 (1964).
- ⁹ An exception is the generalization to $S > 1/2$ of the pair-permutation Hamiltonian, the so called “exchange model”. This model has been studied using Handscomb’s method; Y. C. Chen, H. H. Chen, and F. Lee, Phys. Lett. A **130**, 257 (1988).
- ¹⁰ J. W. Lyklema, Phys. Rev. Lett. **49**, 88 (1982).
- ¹¹ R. Blankenbecler, D. J. Scalapino and R. L. Sugar, Phys. Rev. D **24**, 2278 (1981).
- ¹² D. H. Lee, J. D. Joannopoulos, and J. W. Negele, Phys. Rev. B **30**, 1599 (1984).
- ¹³ S. C. Chakravarty and D. B. Stein, Phys. Rev. Lett., **49**, 582 (1982).
- ¹⁴ M. Suzuki, in Ref. 4.
- ¹⁵ J. W. Negele and H. Orland, *Quantum Many-Particle Systems*, (Addison-Wesley Publishing Co., Redwood City, California, 1988).
- ¹⁶ A. W. Sandvik and J. Kurkijärvi, Phys. Rev. B **43**, 5950 (1991).
- ¹⁷ A. W. Sandvik, J. Phys. A **25**, 3667 (1992).
- ¹⁸ N. V. Prokofev, B. V. Svistunov, and I. S. Tupitsyn, preprint (cond-mat/9703200); Zh. Eks. Teor. Fiz. **64**, 853 (1996) (translation in cond-mat/9612091).
- ¹⁹ B. B. Beard and U.-J. Wiese, Phys. Rev. Lett. **77**, 5130 (1996).
- ²⁰ H. G. Evertz, G. Lana, and M. Marcu, Phys. Rev. Lett. **70**, 875 (1993).
- ²¹ R.-H. Swendsen and J.-S. Wang, Phys. Rev. Lett. **58**, 86 (1987).
- ²² M. Hase, I. Terasaki, and K. Uchinokura, Phys. Rev. Lett. **70**, 3651 (1993);
- ²³ M. Ysobe and Y. Ueda, J. Phys. Soc. Jpn. **65**, 1178 (1996).
- ²⁴ A. W. Sandvik and D. K. Campbell (work in progress).
- ²⁵ A. W. Sandvik, in *Numerical Methods for Lattice Many-Body Models*, ed. by D. J. Scalapino (to be published).
- ²⁶ A. W. Sandvik, A. V. Chubukov, and S. Sachdev, Phys. Rev. B **51**, 16483 (1995). A. W. Sandvik and D. J. Scalapino, Phys. Rev. B **53**, R526 (1996).
- ²⁷ A. W. Sandvik, Phys. Rev. B **52** R9831 (1995).
- ²⁸ O. A. Starykh, A. W. Sandvik, and R. R. P. Singh (to appear in Phys. Rev. B, June 1997).
- ²⁹ A. W. Sandvik, D. J. Scalapino, and P. Henelius, Phys. Rev. B **50**, 10474 (1994).
- ³⁰ A. W. Sandvik and A. Sudbø, Europhys. Lett. **36**, 443 (1996); Phys. Rev. B **54**, R3746 (1996).
- ³¹ E. Y. Loh Jr. *et al.*, Phys. Rev. B **41**, 9301 (1990).
- ³² S. Miyashita, M. Takasu, and M. Suzuki in Ref. 4.
- ³³ J. Boucher and L. P. Regnault, J. Phys. I (France) (to be published); P. H. M. van Loosdrecht *et al.*, Phys. Rev. Lett. **78**, 487 (1997).
- ³⁴ Y. Fuji *et al.*, J. Phys. Soc. Jpn. **66**, 326 (1997); M. Weiden *et al.*, preprint (cond-mat/9703052).
- ³⁵ J. Riera and A. Dobry, Phys. Rev. B **51**, 16098 (1995); G. Castilla, S. Chakravarty, and V. J. Emery, Phys. Rev. Lett. **75**, 1823 (1995).
- ³⁶ D. Augier, D. Poilblanc, S. Haas, A. Delia, and E. Dagotto, preprint (cond-mat/9704015).
- ³⁷ K. Fabricius, A. Klümber, U. Löw, B. Büchner, and T. Lorenz, preprint (cond-mat/9705036).
- ³⁸ It has recently been noted that as $T \rightarrow 0$, results in the zero winding number sector become exact even for a finite system; P. Henelius *et al.* (unpublished).
- ³⁹ S. Eggert, I. Affleck, and M. Takahashi, Phys. Rev. Lett. **73**, 332 (1994).
- ⁴⁰ D. Augier and D. Poilblanc, preprint (cond-mat/9705032).
- ⁴¹ J. E. Hirsch and E. Fradkin, Phys. Rev. **27**, 4302 (1983); E. Fradkin and J. E. Hirsch, Phys. Rev. B **27**, 1680 (1983).
- ⁴² M. C. Cross and D. S. Fisher, Phys. Rev. B **19**, 402 (1979).
- ⁴³ D. C. Johnston, Phys. Rev. B **54**, 13009 (1996).
- ⁴⁴ S. Eggert, Phys. Rev. B **53**, 5116 (1996).
- ⁴⁵ P. C. Hohenberg and W. F. Brinkman, Phys. Rev. B **10**, 128 (1974).
- ⁴⁶ M. Greven, R. J. Birgeneau, and U. J. Wiese, Phys. Rev. Lett. **77**, 1865 (1996); B. Frischmut, B. Ammon, and M. Troyer, Phys. Rev. B **54**, R3714 (1996). M. Troyer, Zhitomirsky, and K. Ueda, Phys. Rev. B **55**, R6117 (1997).
- ⁴⁷ N. Kawashima, J. E. Gubernatis, and H. G. Evertz, Phys. Rev. B **50**, 136 (1994).
- ⁴⁸ N. Kawashima, J. Stat. Phys. **82**, 131 (1996).

q/π	$S(q)$ (QMC)	$S(q)$ (exact)	$\chi(q)$ (QMC)	$\chi(q)$ (exact)
0	0.008581(24)	0.008590	0.06864(20)	0.068720
1/6	0.048110(5)	0.048120	0.11822(3)	0.118266
1/3	0.102865(8)	0.102875	0.14422(3)	0.144236
1/2	0.169906(13)	0.169917	0.19746(5)	0.197478
2/3	0.263758(18)	0.263768	0.32669(8)	0.326648
5/6	0.43371(5)	0.433742	0.8027(3)	0.803118
1	0.95472(18)	0.954566	3.9897(13)	3.989397

TABLE I. Simulation results for the static structure factor and the static susceptibility of a 12-site Heisenberg chain at $\beta = 8$, compared with the exact results. The numbers within parentheses indicate the statistical errors (defined as one standard deviation of the averages), i.e. 0.123(45) stands for 0.123 ± 0.045 .

FIG. 1. A configuration generated for an 8-site periodic system with $\Delta = 1$ at $\beta = 4$. A row represents a spin state $|\alpha(p)\rangle$, with $p = 0$ to $p = L$ from top to bottom. Solid and open circles indicate up and down spins, respectively. Dashed and solid bars represent operators $[1, b]$ and $[2, b]$, and their associated times are graphed to the right.

FIG. 2. Upper panel: The uniform magnetic susceptibility (in units of $1/J$) of a 128-site Heisenberg chain calculated using the new QMC method (circles with error bars) compared with the exact result for the infinite system (curve). Lower panel: The relative deviation $(\chi_{\text{QMC}} - \chi_{\text{exact}})/\chi_{\text{exact}}$ of the QMC data from the exact result. The solid and open circles are for grand canonical and canonical simulations, respectively.

FIG. 3. Upper panel: The truncation L vs. the number of MC steps performed during the initial parts of two simulations of a 128 site system at $\beta = 8$. In one case (solid curve), all the times were simultaneously updated, whereas in the other case (dashed curve) the times were consecutively updated one-by-one.

FIG. 4. The autocorrelation function for E (solid squares), $\chi(0)$ (open squares), $\chi(\pi)$ (solid circles), and $S(\pi)$ (open circles), obtained in a simulation of a 128-site system at inverse temperature $\beta = 8$.

FIG. 5. The temperature dependence of the effective spin-spin coupling (upper panel), and the size of its RMS fluctuation (lower panel).

FIG. 6. The spin susceptibility (in units of $1/J$) vs. wave-number in the long-wavelength regime for a system with $N = 128$ at inverse temperatures $\beta = 16$ (solid circles), $\beta = 32$ (open circles), $\beta = 64$ (solid squares), and $\beta = 128$ (open squares). The statistical errors are at most the size of the symbols.

FIG. 7. The uniform susceptibility [in units of $1/J_{\text{eff}}(0)$] vs. temperature [in units of $J_{\text{eff}}(0)$], compared with the exact Heisenberg result (solid curve). For the Heisenberg chain $J_{\text{eff}} = J = 1$. The dashed curve is the Heisenberg susceptibility for $J = 0.86 \times J_{\text{eff}}(0)$ and a g -factor ≈ 1.82 . The inset shows the QMC data graphed on the temperature scale set by the temperature dependent coupling $J_{\text{eff}}(T)$ [χ here also contains this factor, i.e., it is given in units of $1/J_{\text{eff}}(T)$], compared with $\chi(T)$ for the Heisenberg chain.

FIG. 8. The staggered susceptibility [in units of $1/J_{\text{eff}}(0)$] vs. temperature (solid circles), compared with results for the Heisenberg chain (open circles). The curve indicates the asymptotic divergent form for the Heisenberg chain.

FIG. 9. The static phonon structure factor vs. wave number at $T/J = 1.0$ (open circles), $T/J = 0.5$ (solid circles), $T/J = 0.25$ (open squares), and $T/J = 0.125$ (solid squares). The corresponding susceptibilities, multiplied by T/J , are indicated by the (in some cases barely visible) solid curves. The statistical errors of the susceptibilities are considerably smaller than those of the structure factors, and are not indicated for sake of clarity. The dashed lines indicate the q -independent structure factors of independent harmonic oscillators at the corresponding temperatures.

FIG. 10. Upper bound (in units of the bare exchange J) for the lowest phonon excitation vs. momentum for a 128-site system at $T = J/64$. The dashed line indicates the bare, momentum independent phonon frequency $\omega_0/J = 0.1$.

FIG. 11. The staggered phonon structure factor vs. inverse temperature for systems of size $N = 8$ (solid circles), $N = 32$ (open circles), and $N = 128$ (solid squares). The statistical errors are smaller than the symbols.

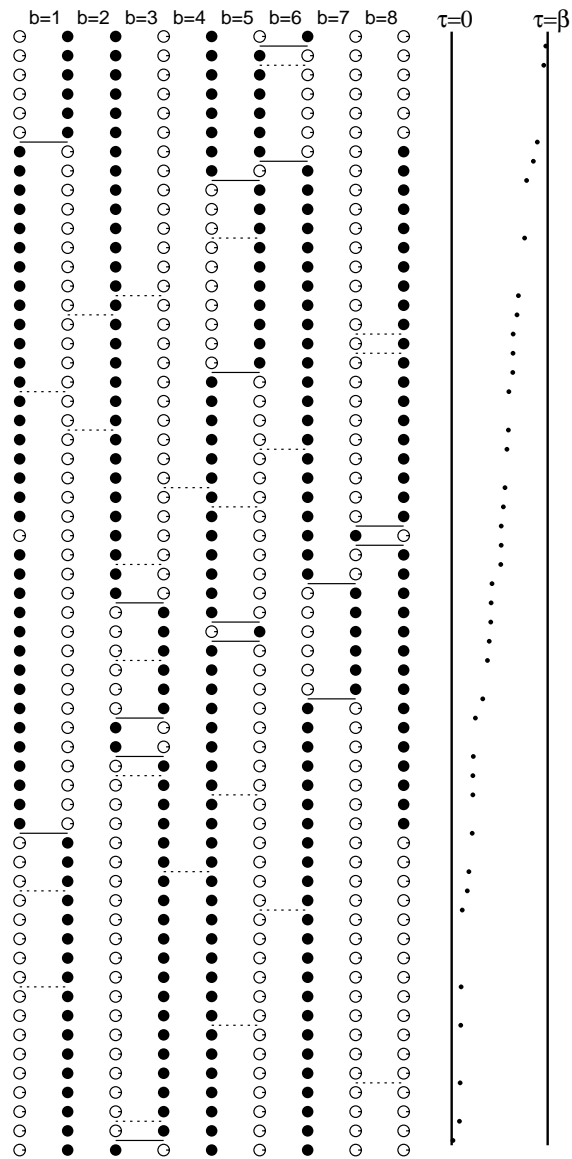


Fig. 1. A. W. Sandvik, R. R. P. Singh, and D. K. Campbell

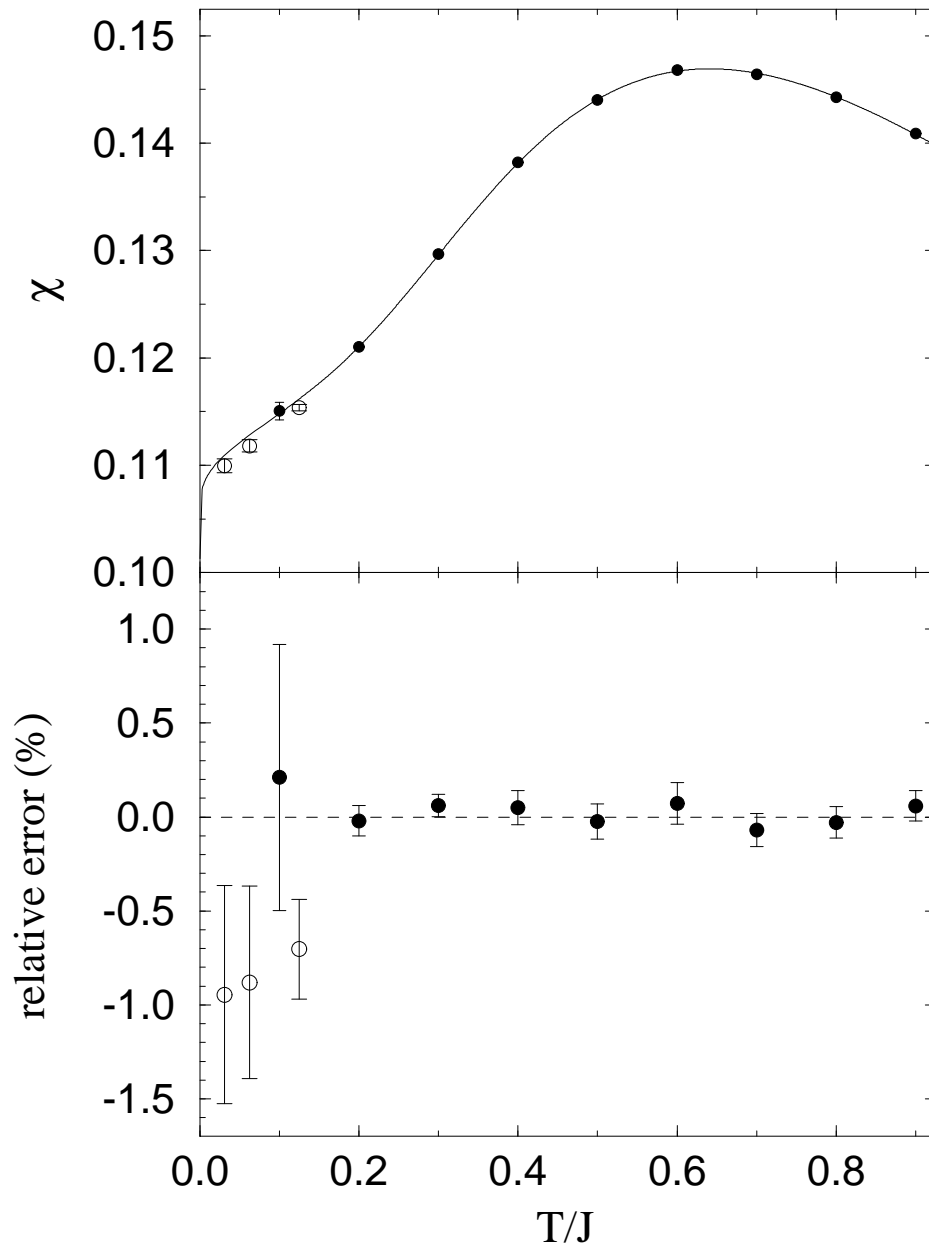


Fig. 2. A. W. Sandvik, R. R. P. Singh, and D. K. Campbell

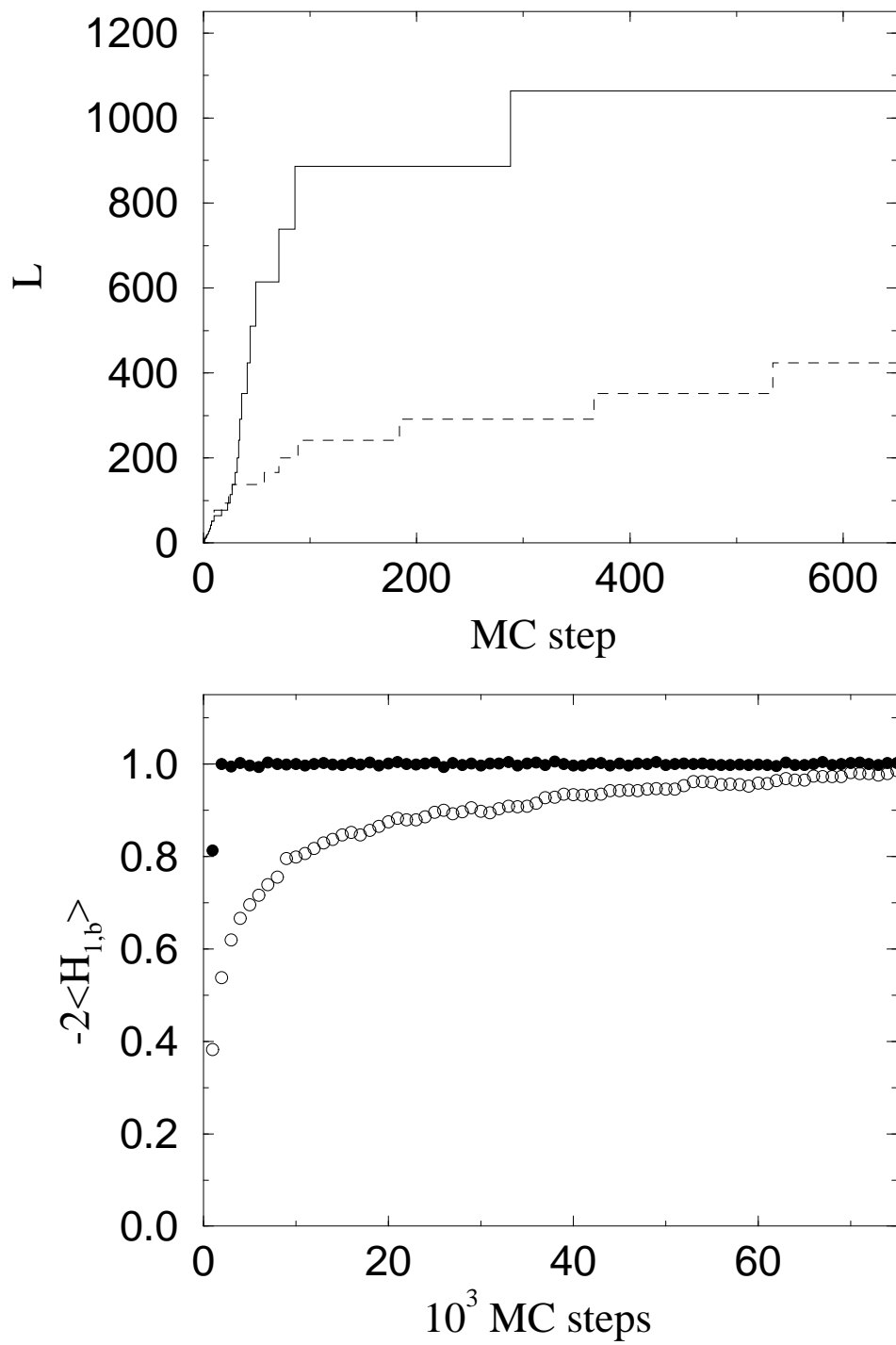


Fig. 3. A. W. Sandvik, R. R. P. Singh, and D. K. Campbell

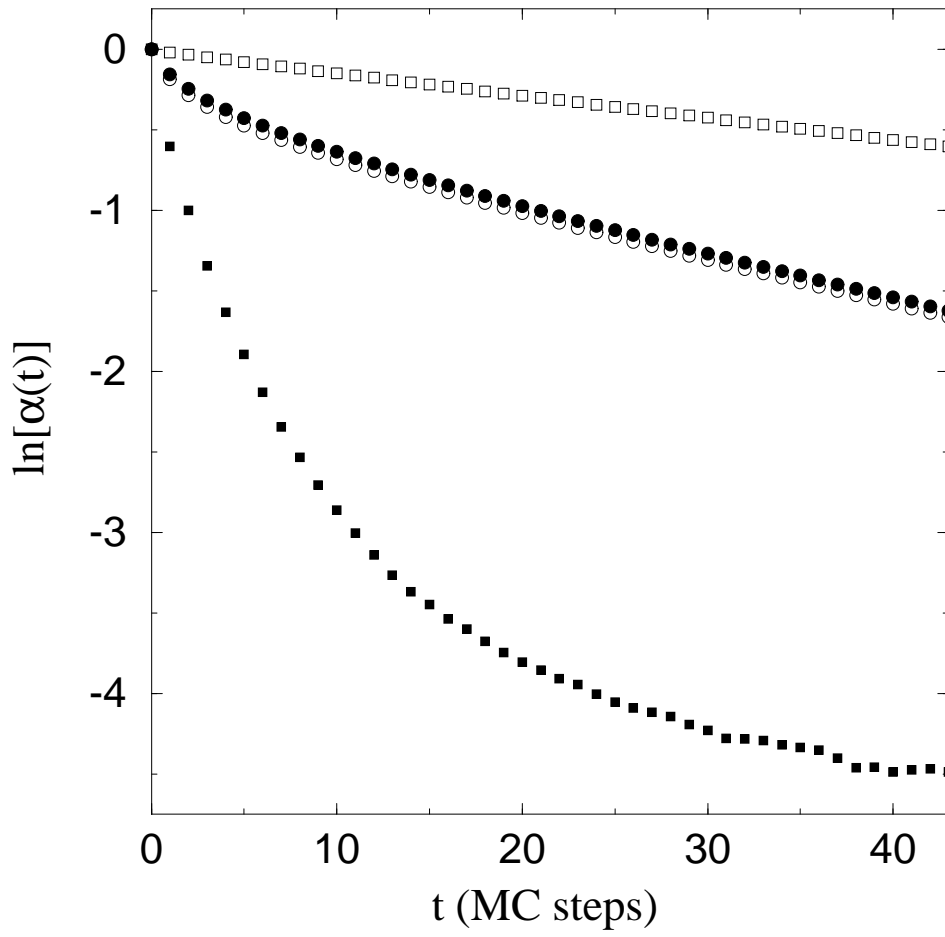


Fig. 4. A. W. Sandvik, R. R. P. Singh, and D. K. Campbell

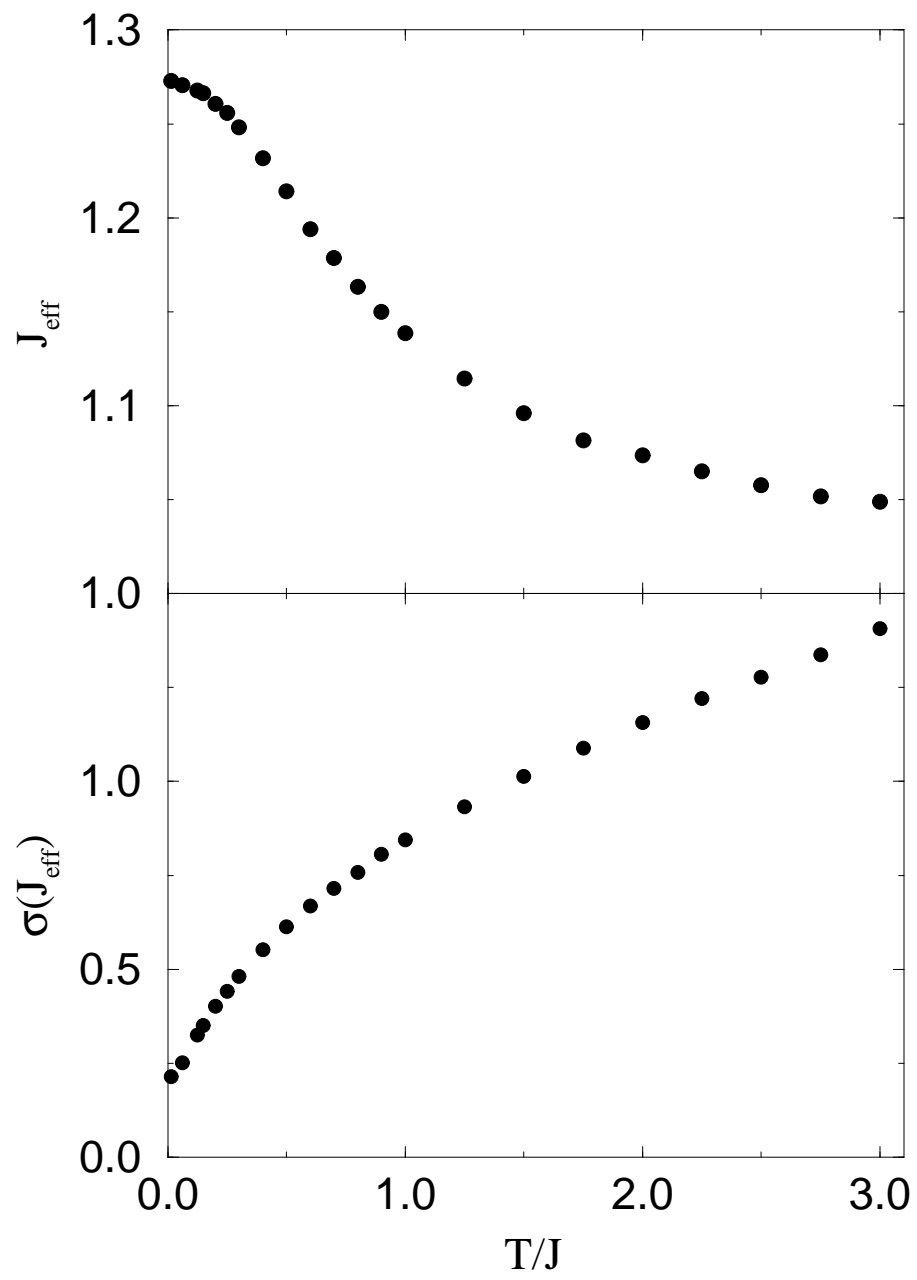


Fig. 5. A. W. Sandvik, R. R. P. Singh, and D. K. Campbell

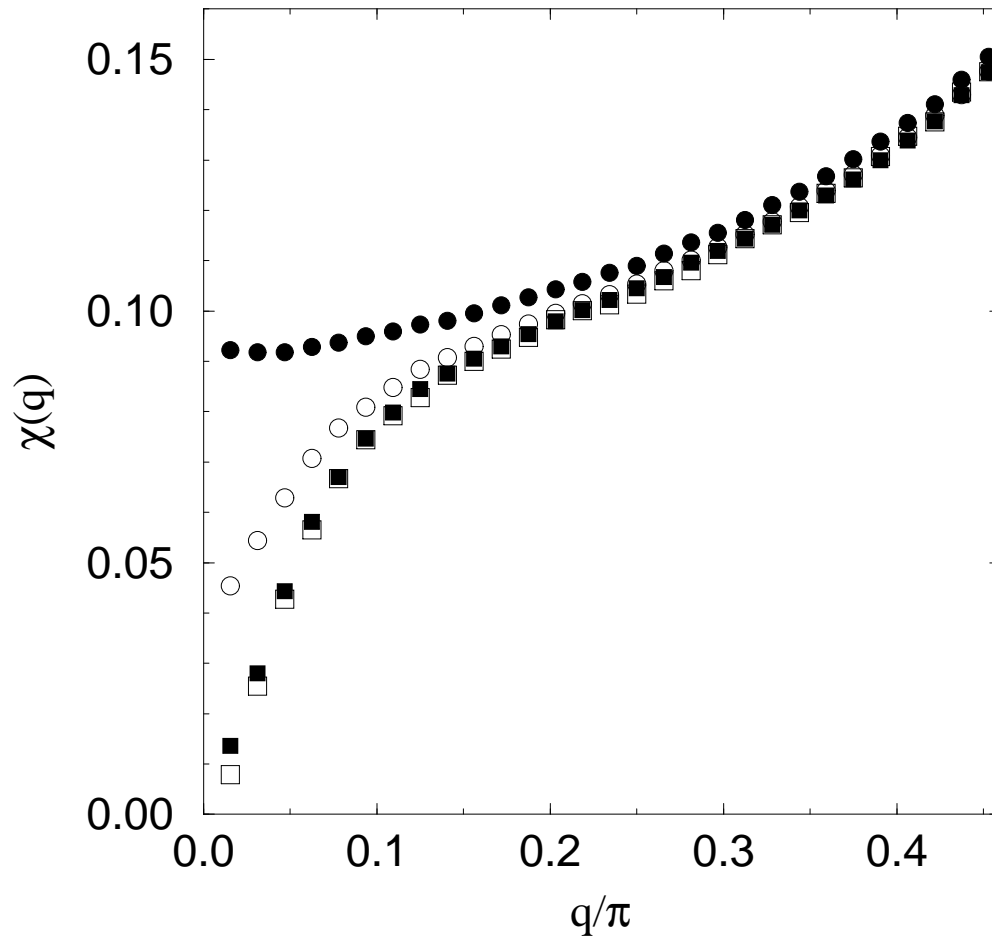


Fig. 6. A. W. Sandvik, R. R. P. Singh, and D. K. Campbell

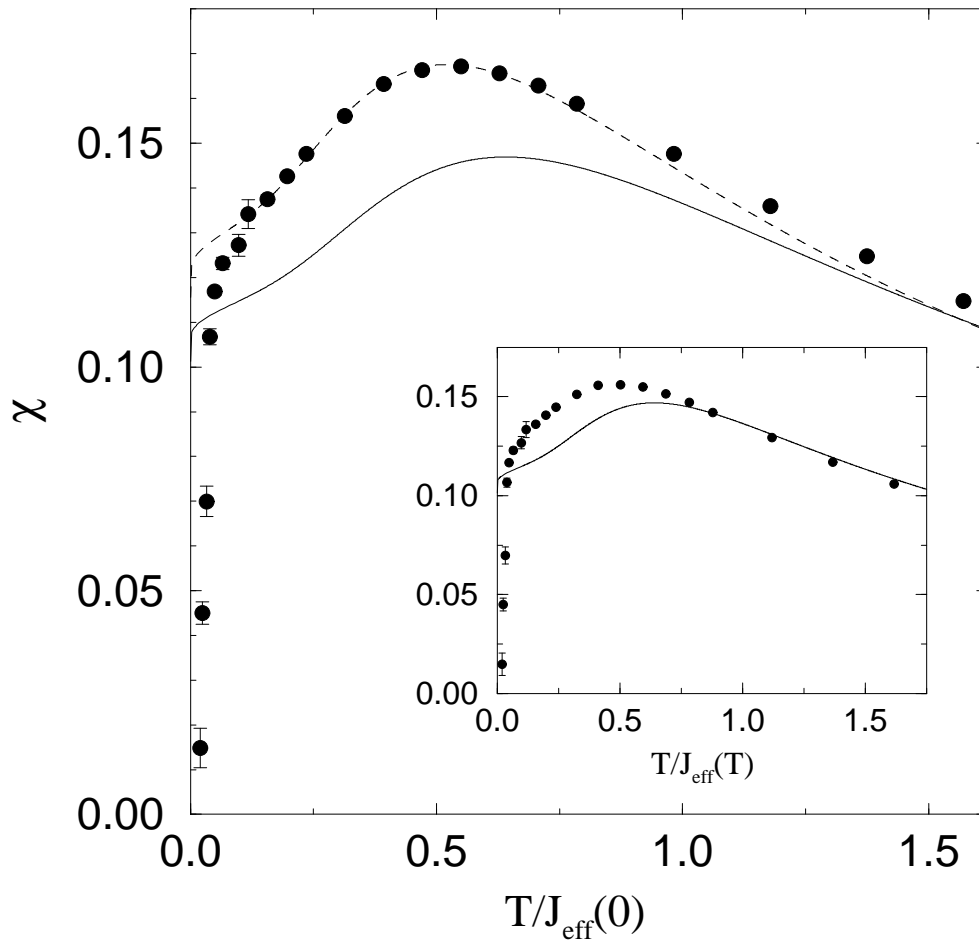


Fig. 7. A. W. Sandvik, R. R. P. Singh, and D. K. Campbell

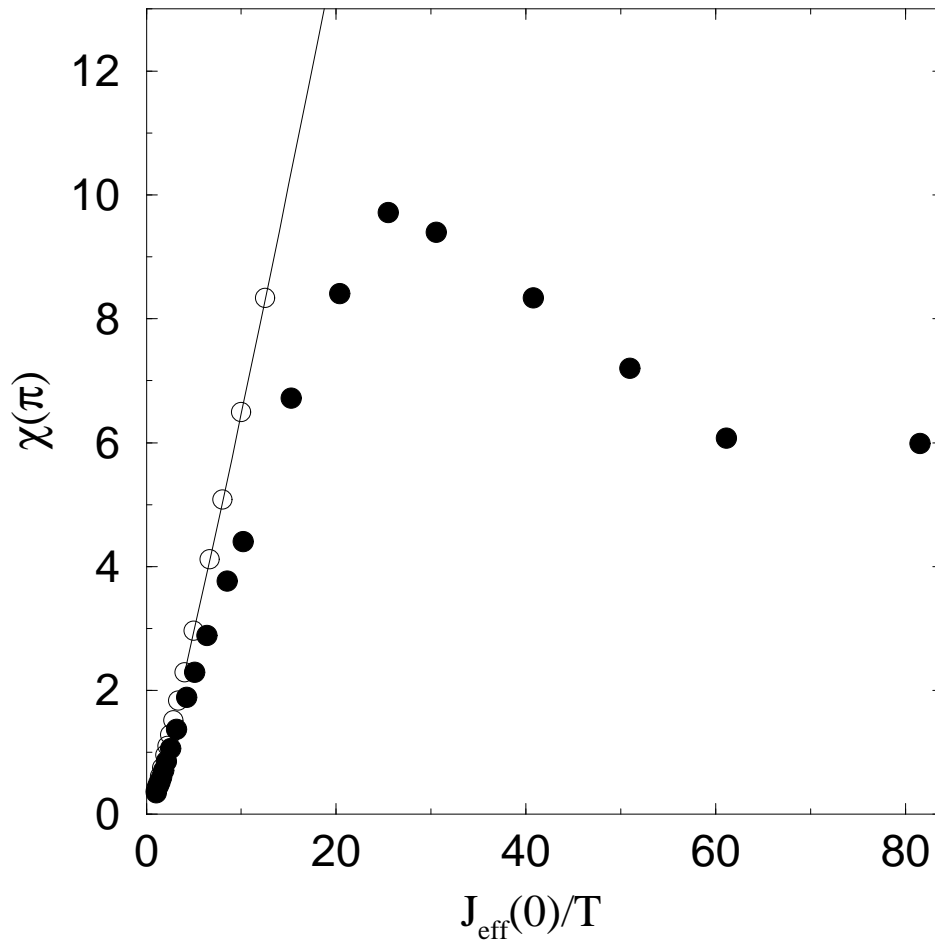


Fig. 8. A. W. Sandvik, R. R. P. Singh, and D. K. Campbell

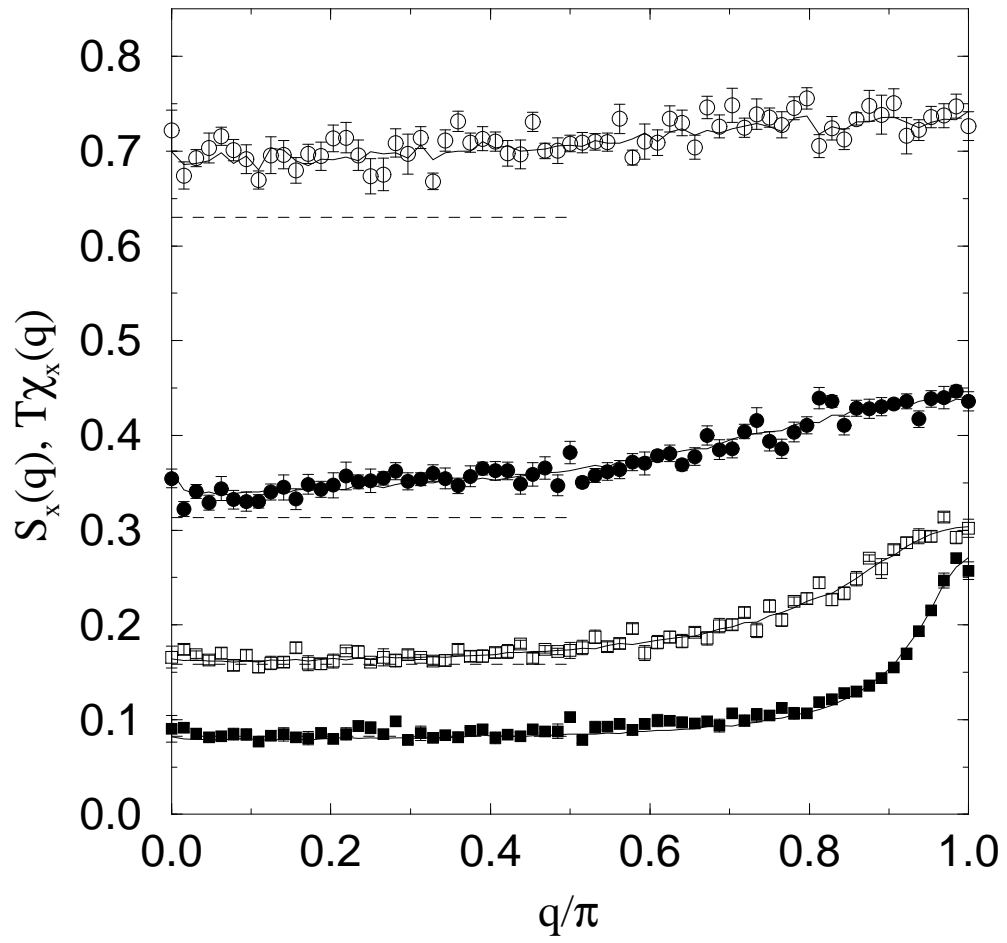


Fig. 9. A. W. Sandvik, R. R. P. Singh, and D. K. Campbell

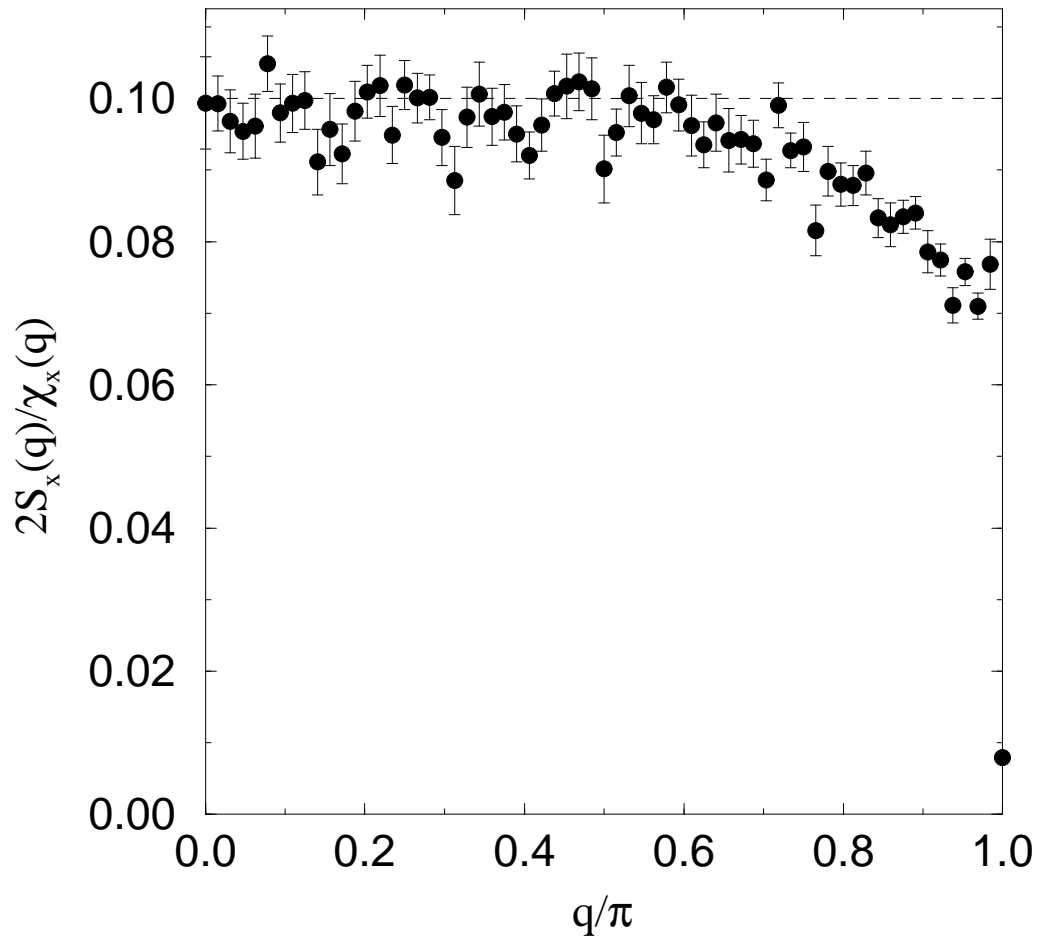


Fig. 10. A. W. Sandvik, R. R. P. Singh, and D. K. Campbell

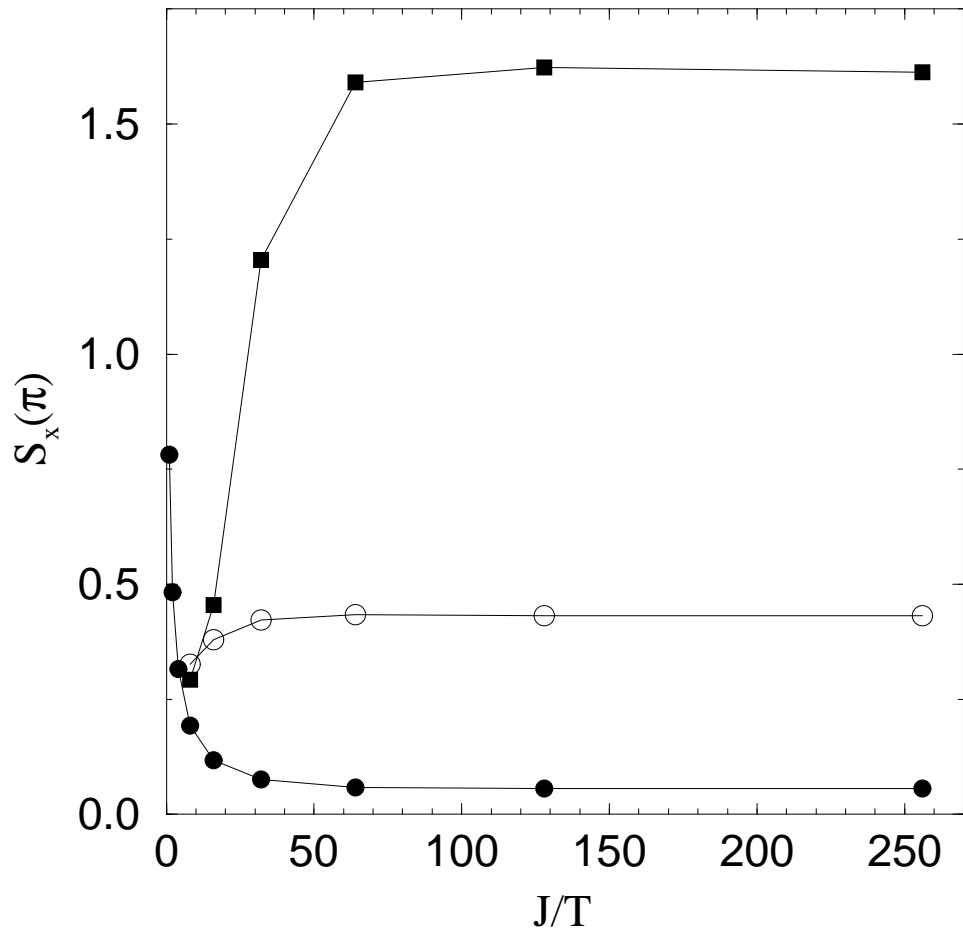


Fig. 11. A. W. Sandvik, R. R. P. Singh, and D. K. Campbell